Zoological Journal of the Linnean Society, 2022, **XX**, 1–24. With 9 figures.

Discovery of a new scale worm (Annelida: Polynoidae) with presumed deep-sea affinities from an anchialine cave in the Balearic Islands (western Mediterranean)

MARÍA CAPA[1], JOAN PONS[2] and DAMIÀ JAUME[2,*]

[1]*Departament of Biology, Universitat de les Illes Balears, 07122 Palma, Illes Balears, Spain*
[2]*IMEDEA (CSIC-UIB), Mediterranean Institute for Advanced Studies, 07190 Esporles, Illes Balears, Spain*

Received 1 June 2021; revised 21 April 2022; accepted for publication 5 May 2022

A remarkable new genus and species of scale worm (Annelida: Polynoidae) was found on the bottom sediments of an anchialine cave on the island of Mallorca (Balearic Islands, western Mediterranean). Specimens reach up to 2 cm long, lack eyes and body pigmentation except for a few scattered minute speckles and show enlarged parapodia and sensorial appendages. A red brain is visible through the translucent tegument. Morphological features resemble those of Eulagiscinae, currently comprising eight species in three genera. Phylogenetic analyses of mitochondrial and nuclear DNA sequences are not conclusive on the position of the new taxon but affinity to Eulagiscinae is not ruled out, particularly when taxa with missing data or non-homologous insertion sites are excluded from the analyses. ***Pollentia perezi* gen. & sp. nov.** is characterized by a unique set of morphological features: 13 pairs of dorsal elytra; a single type of notochaetae (stout, with spinous rows and pointed tip); and two types of neurochaetae (superior flattened, spinous with tridentate tip; inferior shorter and thinner, lanceolate and pectinate). Some characteristics, such as the long parapodial appendages and swimming habits, are shared with other cave scale worms. However, the new taxon is not closely related to the other two known cave-dwelling polynoids.

ADDITIONAL KEYWORDS: adaptation – cave worms – diversity – new genus – new species – Mallorca.

INTRODUCTION

Scale worms (Aphroditiformia) are a diverse group of errant, mainly marine annelids characterized by the display of segmental scales over the dorsum (Zhang *et al.*, 2018), although in some groups, such as members of *Pisione* Grube, 1857, such scales are secondarily lost (Struck *et al.*, 2005; Wiklund *et al.*, 2005; Gonzalez *et al.*, 2018a).

Polynoidae is the most species-rich family of scale worms, including ~900 species, of which nearly half represent monotypic genera (Wehe, 2006; Norlinder *et al.*, 2012; Martin *et al.*, 2021; Read & Fauchald, 2021). The monophyly of the family has been assessed through molecular analyses, but there are no unequivocal morphological apomorphies supporting it (Norlinder *et al.*, 2012; Gonzalez *et al.* 2018a; Zhang *et al.*, 2018). As many as 21 subfamilies of Polynoidae have been recognized (e.g. Wehe, 2006), although several were found to be paraphyletic based on recent molecular studies (Bonifácio & Menot, 2019; Gonzalez *et al.*, 2018a). Monophyly and relationships among these subfamilies remain unresolved, because results of evolutionary analyses vary widely depending on taxon sampling and the number and type of morphological features and molecular markers considered (Gonzalez *et al.*, 2018a, b; Zhang *et al.*, 2018; Bonifácio & Menot, 2019).

Most polynoids are marine benthic and inhabit a wide variety of environments, ranging from the intertidal to the deep sea (e.g. Pettibone, 1967, 1976, 1984, 1985; Chevaldonné *et al.*, 1998; Sui & Li, 2017; Zhang *et al.*, 2018; Bonifácio & Menot, 2019; Wu *et al.*, 2019), and from full-strength marine to brackish waters (Hutchings & Murray, 1984; Martin *et al.*, 2021). Some holopelagic species are also known (Dales & Peter, 1972; Allentoft-Larsen *et al.*, 2021), whereas

*Corresponding author. E-mail: damiajaume@imedea.uib-csic.es
[Version of record, published online 30 July 2022; http://zoobank.org/ urn:lsid:zoobank.org:pub:551AB3FF-DB0B-425D-A3DA-C64537F92876]

several live as symbionts of other organisms (Jumars *et al.*, 2015; Martin & Britayev, 2018; Martin *et al.*, 2021). Despite their broad range of habitats and environmental tolerance, the presence of polynoids in anchialine caves is exceptional. Only *Gesiella jameensis* (Hartmann-Schröder, 1974), known only from a lava tube and adjacent crevicular habitats on Lanzarote (Canary Islands), and *Pelagomacellicephala iliffei* Pettibone, 1985, described from anchialine caves of the Caicos and Great Bahama Bank in the Caribbean (Hartmann-Schröder, 1974; Pettibone, 1985; Gonzalez *et al.*, 2017), are known to occur in this highly demanding environment, characterized by total darkness, lack of photosynthesis, limited exposure to atmospheric oxygen and reduced organic nutrient cycling (Iliffe, 2000). Both taxa share several features presumed to be adaptations to the cave environment, such as swimming habits and presence of long dorsal parapodial cirri (Gonzalez *et al.*, 2018b, 2021). Others, such as the absence of eyes and of body pigmentation, are shared with deep-sea forms (Gonzalez *et al.*, 2018a). The cavernicolous habits of these two polynoids and their affinity to deep-sea taxa led some authors to propose a deep-sea origin for some members of the cave fauna present on oceanic islands (Iliffe *et al.*, 1984; Hart *et al.*, 1985). In fact, recent molecular phylogenetic analyses show *Pelagomacellicephala iliffei* and *Gesiella jameensis* to be sister taxa and place them confidently within the deep-sea subfamily Macellicephalinae Hartmann-Schröder, 1971 (Gonzalez *et al.*, 2018b; Zhang *et al.*, 2018).

Herein, we describe a third new genus and species of anchialine cave polynoid from the island of Mallorca (Balearic Islands, western Mediterranean). We assess its phylogenetic relationships based on morphological traits and on mitochondrial and nuclear sequences, and we highlight the morphological features shared with the other two known cave-dwelling polynoids.

MATERIAL AND METHODS

Study area

The cave where the worms were collected is located on the promontory that separates the bays of Pollença and Alcúdia, on the north coast of Mallorca; Fig. 1A). The cave opens at sea level on a Mesozoic limestone sea cliff and consists of a narrow subaerial passage ~60 m long that connects to a small chamber occupied by a brackish-water lake. This lake represents the entrance to a submarine chamber (not shown in Fig. 1B) that reaches a maximum depth of 29 m. The water column of the lake is permanently stratified, with a sharp pycnocline developed at ~11 m depth, with full-strength marine water (38 PSU) immediately below (Fig. 1C). The cave records a palaeo-sea level at 13 m depth in the form of a phreatic overgrowth on speleothems and cave walls, denoting the long-term transitory nature of the aquatic cave habitat. The bottom of this chamber mostly consists of bare rock, with some patches of calcareous silt.

Specimen collection and fixation

Only three specimens were found after two collecting trips to the cave (on 11 March 2019 and 3 June 2020). They were observed crawling on bottom sediments and kept alive in jars until their study in the laboratory a few hours later. Two specimens were fixed in 96% ethanol (kept at 4–6 °C) and a third one in RNAlater (Thermo Fisher Scientific, Waltham, MA, USA) to be used in subsequent transcriptomic studies. Several other visits to the cave reported no further individuals.

Morphological analyses

Specimens were examined under both stereo- and compound light microscopes. Photographs were taken with a Euromex DC.18000-PRO camera attached to a Euromex DZ.1105 stereomicroscope. Methyl Blue was used to stain specimens and enhance the contrast of some structures. A mid-longitudinal section was made along the ventral side of the anterior end of the paratype (MNCN 16.01/18956) to study the morphology of the pharynx. The anterior end of the paratype was dissected from the rest of the body and sectioned in pieces for further study by scanning electron microscopy (SEM). Some anterior, midbody and posterior parapodia were also dissected for their detailed examination under the SEM. Body fragments were dehydrated in a series of mixtures of absolute ethanol and hexamethyldisilazane (ratios 3:1, 2:2 and 1:3), then put into pure hexamethyldisilazane. Samples were mounted on holders, sputter-coated with gold (10 nm thickness) and examined with a HITACHI S-3400N SEM at the University of the Balearic Islands. Vouchers were deposited at Museo Nacional de Ciencias Naturales (MNCN, Madrid).

Molecular data and analyses

A few dorsal cirri of paratype MNCN 16.01/18956 were taken for DNA extraction. This was performed using QuickExtract (Epicentre Biotechnology, Madison, WI, USA) according to the manufacturer's instructions. Four DNA fragments were amplified by polymerase chain reaction (PCR): two partial mitochondrial genes, corresponding to the cytochrome *c* oxidase subunit I (*COI*) and to the large ribosomal subunit (16S rRNA), and two partial nuclear markers (18S rRNA and 28S

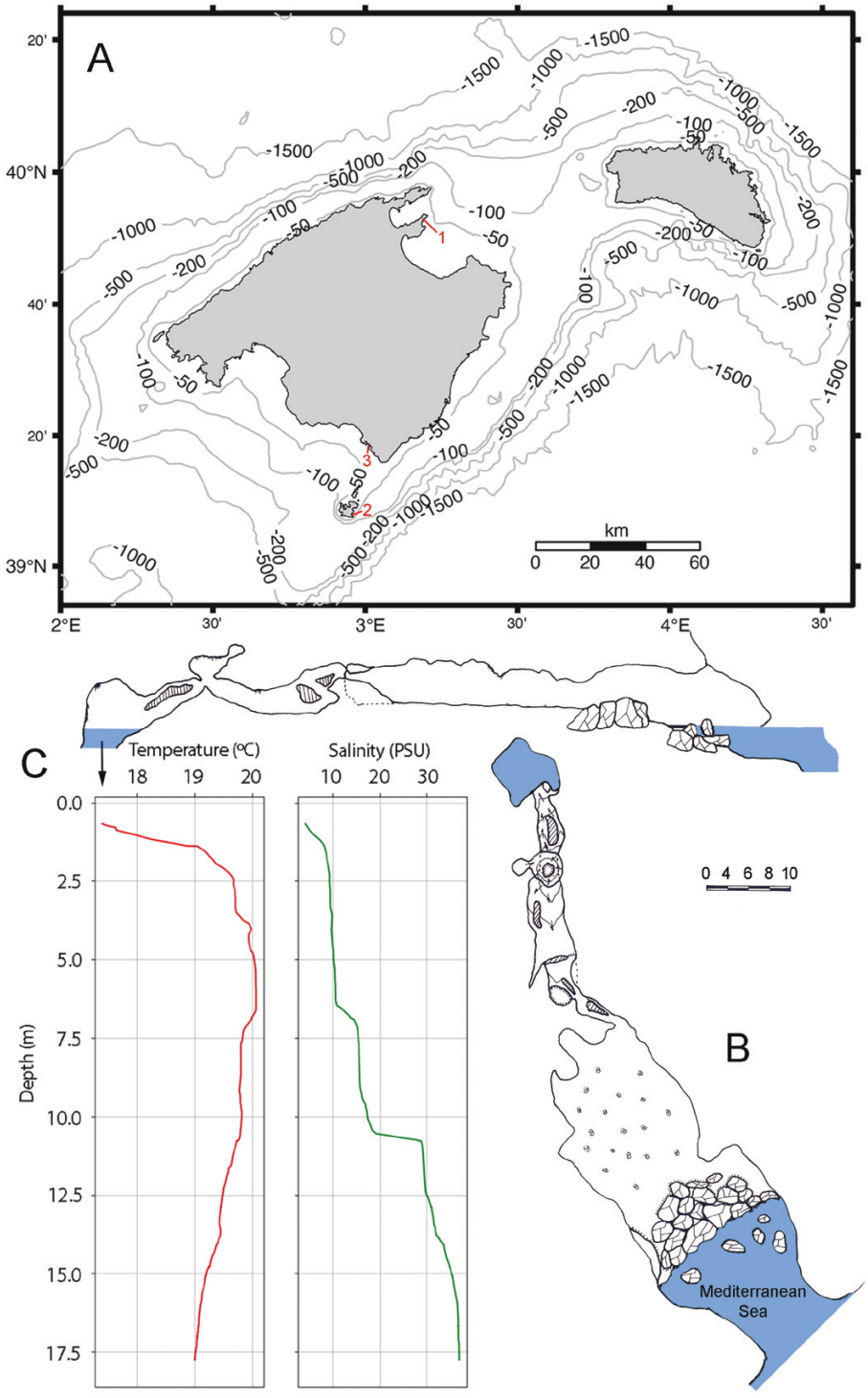

Figure 1. A, map of the Balearic Islands showing the known localities (red numbers) of the new cave polynoid worm *Pollentia perezi* gen. & sp. nov. (1), the stygobiont cirolanid isopod *Metacirolana ponsi* (1 and 2) and the stygobiont mysid *Burrimysis palmeri* (1, 2 and 3); these three taxa occur only in full-strength marine water layers of anchialine caves. B, plan view and section of the cave harbouring the new polynoid (after Suárez, 1993; modified). C, temperature and salinity profiles of the anchialine lake harbouring the new polynoid (notice euhaline conditions below 11 m depth). Temperature, salinity and depth profiles were obtained with an RBR XR-420 conductivity, temperature and depth (CTD) profiler.

rRNA). The amplification reaction of the *COI* sequence contained 10 µL of VWR RedTaq DNA Polymerase Master Mix (VWR International, Haasrode, Belgium; already containing NH_4 + buffer system, dNTPs and magnesium chloride), 0.3 µL of each primer (10 µM) and 1.4 µL of DNA (for a total reaction mixture of 12 µL). For the remaining three markers, reactions contained 10 µL Bioline MyTaqRedMix (Bioline, London, UK; with buffer, DNTPs and $MgCl_2$ incorporated into the mix), 7.4 µL H_2O, 0.8 µL of each primer (10 µM) and 1 µL of DNA (for a total reaction mixture of 20 µL). Primer sequences and cycling conditions are given in Table 1.

The PCR products were run on a 1% agarose gel containing ethidium bromide for 30 min at 80 V and visualized under ultraviolet light. The PCR products with the expected length were cleaned using the kit microCLEAN for PCR clean-up (Microzone, Lewes, UK). Sanger cycle sequencing was performed on both strands at Eurofins Genomics DNA Sequencing Department (Ebersberg, Germany). Forward and reverse reads were merged into consensus sequences and edited using GENEIOUS BASIC (Kearse *et al.*, 2012). *COI* gene sequences were translated into amino acids in SEAVIEW v.4.7 (Gouy *et al.*, 2010) and checked for the presence of stop codons and rare non-synonymous substitutions that could be indicative of the amplification of pseudogenes.

Polynoid sequences of additional species were downloaded from GenBank. Two species of Sigalionidae were considered as outgroups. A list of all specimens considered and their respective sequence accession numbers is presented in Table 2.

A reduced dataset was also considered, in order to estimate the potential impact of missing data in the outcome of phylogenetic analyses. This included a single species per genus for which at least three out of the four markers were available. When several congeners were available, the one with the maximum number of genes and longer sequences was selected (Table 2).

PHYLOGENETIC ANALYSES

The *COI* sequences were aligned at the protein level in MUSCLE v.3.8.1551 (Edgar, 2004) using default parameters, then back-translated to nucleotides in SEAVIEW v.4.7 (Gouy *et al.*, 2010). Ribosomal genes 16S rRNA, 18S rRNA and 28S rRNA were aligned using different programs because some residues are aligned in different positions depending on the models and parameters implemented, particularly when large insertions or deletions occur. Alignment approaches include: (1) MUSCLE using default parameters; (2) MAFFT v.7.397 (Katoh & Standley, 2013) using the *xinsi* option, which considers the secondary structure of RNA in pairwise comparisons using the MXSCARNA algorithm (Tabei *et al.*, 2008); and (3) GUIDANCE2 (http://guidance.tau.ac.il/; Sela *et al.*, 2015), which scores nucleotide positions in the alignment depending on whether residues are confidently aligned using the base alignment built in MAFFT (--maxiterate 10--globalpair) and 100 alignments built from the guide tree obtained from 100 bootstrap replicates of the initial base alignment.

In order to assess the phylogenetic impact produced by poorly aligned positions in both MUSCLE and MAFFT *xinsi* alignments, non-conserved blocks were trimmed in GBLOCKS v.0.91b (Talavera & Castresana, 2007) in low stringent conditions (commands -b2 = 85, -b3 = 8, -b4 = 10, -b5 = h, -t = d, -e = fas and -p = t). In the base GUIDANCE2 alignment, we removed unreliable positions such that trimmed alignments included only fully supported aligned positions (score 100%). In addition, and in order to implement a stricter primary homology criterion (*sensu* de Pinna, 1991), we also removed from the

Table 1. Primers used in this study, with their respective cycles

Marker	Primer	Source	Sequence	Cycle
COI	jgLCO/	(Geller *et al.*, 2013)	TITCIACIAAYCAYAARGAYATTGG	4 min at 95 °C; 35 × (40 s at
	jgHCO	(Geller *et al.*, 2013)	TAIACYTCIGGRTGICCRAARAAYCA	94 °C, 40 s at 48 °C and 60 s at 72 °C); 6 min at 72 °C
16S rRNA	16Sarl	(Palumbi, 1996)	CGCCTGTTTATCAAAAACAT	1 min at 96 °C; 29 × (30 s at
	16SbrH	(Palumbi, 1996)	CCGGTCTGAACTCAGATCACGT	95 °C, 30 s at 52 °C and 60 s at 72 °C); 7 min at 72 °C
18S rRNA	18SA	(Medlin *et al.*, 1988)	AACCTGGTTGATCCTGCCAGT	3 min at 96 °C; 35 × (40 s at
	18SL	(Apakupakul *et al.*, 1999)	CCAACTACGAGCTTTTTAACTG	95 °C, 40 s at 49 °C and 45 s at 72 °C); 5 min at 72 °C
28S rRNA	28SC1	(Lê *et al.*, 1993)	ACCCGCTGAATTTAAGCAT	1 min at 96 °C; 29 × (30 s at
	28SD2	(Lê *et al.*, 1993)	TCCGTGTTTCAAGACGG	95 °C, 1 min at 62 °C and 1 min at 72 °C); 7 min at 72 °C

Table 2. Collection locality of sequenced individuals for the complete dataset, vouchers and GenBank accession numbers. Species included in the reduced dataset are in bold. New sequences of *Pollentia perezi* gen. & sp. nov. are set in bold italic.

Species	Locality	Voucher	18S	28S	16S	*COI*
***Neoleanira tetragona* (outgroup)**	Trondheimsfjord, Norway and Sweden	SMNH118984	AY839570	JN852872	JN852911	AY839582
***Pholoe baltica* (outgroup)**	Sweden	SMNH118985	AY839573	JN852873	JN852912	AY839585
Abyssarya acus	Clarion-Clipperton Fracture Zone, East Pacific	MNHN-IA-TYPE 1811	MH233231	–	MH233179	MH233277
Acholoe astericola	Banyuls, France	SMNH118959/ SMNH73630	AY839567	JN852850	JN852888	AY839576
Alentia gelatinosa	Trondheimsfjord, Norway	–	AY839566	–	–	AY839577
Antarctinoe ferox	Ross Sea	–	–	–	KF713463	KF713373
***Antipathipolyeunoa* sp.**	Atlantis Bank seamount, SW Indian Ridge	–	KU738169	KU738184	KU738149	KU738202
Austropolaria magnicirrata	Pine Island Bay, Amundsen Sea	NHM2012.92	JX863895	–	JX863896	–
Bathyeliasona mariaae	Clarion-Clipperton Fracture Zone, East Pacific	MNHN-IA-TYPE 1815	MH233204	–	MH233149	MH233249
Bathyfauvelia glacigena	Clarion-Clipperton Fracture Zone, East Pacific	MNHN-IA-TYPE 1817	MH233218	–	MH233160	MH233274
Bathyfauvelia ignigena	Clarion-Clipperton Fracture Zone, East Pacific	MNHN-IA-TYPE 1819	MH233246	–	MH233200	MH233262
Bathykurila guaymasensis	Southern California Margin	–	DQ074765	–	–	DQ074766
Bathymoorea lucasi	Clarion-Clipperton Fracture Zone, E Pacific	MNHN-IA-TYPE 1822	MH233223	–	MH233165	MH233266
Bathypolaria sp.	Clarion-Clipperton Fracture Zone, East Pacific	MNHN-IA-PNT 63	MH233206	–	MH233151	MH233281
Branchinotogluma sandersi	Juan de Fuca Ridge	SMNH118960	JN852821	JN852851	JX863896	JN852923
Branchinotogluma elytropapillata	Okinawa Trough	–	MG799378	MG799380	MG799377	MG799389
Branchinotogluma japonicus	Okinawa Trough	CBM ZV 1114	KY753841		KY753824	MG799392
Branchipolynoe pettiboneae	China	–	KU507074	-	MK694872	MG799393
Branchipolynoe symmytilida	East Pacific Rise	–	–	–	AF315055	AY646021
Bruunilla nealae	Clarion-Clipperton Fracture Zone, East Pacific	MNHN-IA-TYPE 1824	MH233216	–	MH233158	–
***Bruunilla* sp.**	Clarion-Clipperton Fracture Zone, East Pacific	MNHN-IA-PNT 72	MH233247	–	MH233201	MH233263
Bylgides elegans	Sweden	SMNH118962	JN852822	JN852852	JN852890	JN852924
Bylgides sarsi	Sweden	SMNH118961	JN852823	JN852853	JN852891	JN852925
Capitulatinoe* cf. *cupisetis	Gulf of Thailand	–	KF919301	KF919302	KF919303	–
Eulagisca gigantea	Amundsen Sea	–	MG905040	–	KJ676608	KJ676633
Eunoe nodosa	Norway	SMNH118963	JN852824	JN852854	JN852892	JN852926
Gastrolepidia clavigera	Papua New Guinea	SMNH118964	JN852825	JN852855	JN852893	JN852927

Table 2. Continued

Species	Locality	Voucher	18S	28S	16S	*COI*
Gattyana ciliata	–	–	AY894297	DQ790035	-	XXX
Gattyana cirrhosa	Sweden	SMNH118965	JN852826	JN852856	JN852894	JN852928
Gesiella jameensis	Canary Islands	–	KY454403	KY823476	KY454412	KY454429
Gorgoniapolynoe corralophila	Atlantis Bank seamount, SW Indian Ridge	–	KU738175	KU738192	KU738157	KU738209
Halosydna brevisetosa	California	SMNH118966	JN852827	JN852857	–	AY894313
Halosydnella australis	Pontal do Sul, Brazil	–	KY823449	KY823463	KY823480	KY823495
Harmothoe glabra	England	SMNH118967	JN852828	JN852858	JN852896	JN852929
Harmothoe imbricata	Bohuslan, Sweden		AY340434	AY340400	AY340463	AY839580
Harmothoe impar	Sweden	SMNH118968	JN852829	JN852859	JN852897	JN852930
Harmothoe oculinarum	Trondheim, Norway	SMNH118969	AY894299	JN852860	JN852898	AY894314
Harmothoe rarispina	Disko Island, Greenland		KY657611	KY657624	KY657641	KY657659
Hermenia verruculosa	Belize	SMNH118970	JN852830	JN852861	JN852899	JN852931
Hodor anduril	Clarion-Clipperton Fracture Zone, East Pacific	MNHN-IA-TYPE 1826	MH233240	–	MH233191	MH233288
Hodor hodor	Clarion-Clipperton Fracture Zone, East Pacific	MNHN-IA-TYPE 1825	MH233238	–	MH233189	MH233257
Hyperhalosydna striata	Japan	SMNH118971	JN852831	JN852862	JN852900	JN852932
Intoshella dictyaulus	Near the Mariana Trench	–	MG519807	–	–	MG519808
Lepidasthenia elegans	France	SMNH118973	–	JN852863	JN852901	JN852933
***Lepidonotopodium* sp.**	–		KY753842	KY753842	KY753828	KY753828
Lepidonotus clava	England	SMNH118974	JN852833	JN852864	JN852902	JN852934
Lepidonotus squamatus	Sweden	SMNH118975	AY894300	JN852865	JN852903	AY894316
Lepidonotus sublevis	Griffin Bay, Western Australia	USNM107222	AY894301	DQ790039	–	AY894317
Levensteiniella undomarginata	Okinawa Trough	CBM ZV 1118	MG799379	MG799381	MG799376	MG799385
Macellicephala clarionensis	Clarion-Clipperton Fracture Zone, East Pacific	MNHN-IA- 1828	–	–	MH233183	MH233269
Macellicephala parvafauces	Clarion-Clipperton Fracture Zone, East Pacific	MNHN-IA-TYPE 1830	MH233225	–	MH233173	MH233275
Macellicephala brenesorum	Admundsen Sea, Southern Ocean	NHMUK:2018.830	MG905041	–	MG905035	MG905047
Macellicephala violacea	–	NHMUK:2012.12	MG905046	–	MG905038	JX119016
Malmgreniella mcintoshi	Sweden	SMNH118976	JN852834	JN852866	JN852904	JN852935
Melaenis loveni	Svalbard, Norway	SMNH118977	JN852835	JN852867	JN852905	JN852936
Neopolynoe paradoxa	Norway	SMNH118978	JN852836	JN852868	JN852906	JN852937
Neopolynoe acanellae	Cantabric Sea; Spain	–	MN653050	MN653123	MN653064	MN656076
Neopolynoe chondrocladiae	Cantabric Sea; Spain	–	MN653051	MN653124	–	MN656104
Paradyte crinoidicola	Papua New Guinea	SMNH118979	JN852837	JN852869	JN852907	JN852938
Paralepidonotus ampulliferus	Papua New Guinea	SMNH118980	JN852838	AF185164	JN852908	JN852939

Table 2. Continued

Species	Locality	Voucher	18S	28S	16S	*COI*
Pelagomacellicephala iliffei	Eleuthera, Bahamas	–	KY454408	KY823474	KY454420	KY454435
Polaruschakov lamellae	Clarion-Clipperton Fracture Zone, East Pacific	MNHN-IA-TYPE 1837	MH233205	–	MH233150	MH233250
Polaruschakov limaae	Clarion-Clipperton Fracture Zone, East Pacific	MNHN-IA-TYPE 1840	MH233237	–	MH233187	–
Polaruschakov omnesae	Clarion-Clipperton Fracture Zone, East Pacific	MNHN-IA-TYPE 1841	MH233213	–	MH233155	MH233283
Pollentia perezi	Alcúdia, Balearic Islands	*MNCN 16.01/18956*	***OU070105***	***OU070127***	***OU070128***	***OU070106***
Polyeunoa laevis	Ross Sea	–	–	–	KF713464	KF713377
Polynoe scolopendrina	England	SMNH118981	JN852839	JN852870	JN852909	JN852940
Robertianella synophthalma	Cantabric Sea; Spain	–	MN653053	MN653126	MN653122	MN656132
Thormora jukesii	Japan	SMNH118983	JN852840	JN852871	JN852910	JN852941
Yodanoe desbruyeresi	Clarion-Clipperton Fracture Zone, East Pacific	MNHN-IA-TYPE 1843	–	–	MH233156	MH233251
Yodanoe sp.	Clarion-Clipperton Fracture Zone, East Pacific	MNHN-IA-PNT 73	–	–	MH233195	MH233273

Table 3. Alignment strategies followed for the different markers

Software	*COI*	16S rRNA	28S rRNA	18S rRNA
MUSCLE	All positions	All positions or removed non-conserved positions in GBLOCKS		
MAFFT	NA	All positions or removed non-conserved positions in GBLOCKS		
GUIDANCE2	NA	100%		

Selected parameters and details of software versions are provided in the main text.
Abbreviation: NA, not applicable.

GUIDANCE2 alignment those insertions present in a single sequence (autapomorphies) because they have no phylogenetic signal. A summary of the alignment approaches is shown in Table 3. Alignments and the resulting phylogenetic topologies of the four markers concatenated are given in the Supporting Information (S1–6).

A total of 77 species were included in the initial complete phylogenetic analyses, together with the new species described herein (Table 2). Sequences from the four markers were concatenated, and alignments contained 711 bp for *COI*, with 325 parsimony-informative sites (103 for first plus second codon positions and 222 for third codon sites). The length and number of parsimony sites of ribosomal genes 16S rRNA, 18S rRNA and 28S rRNA varied depending on the alignment program implemented and the removal of the poorly aligned regions in GBLOCKS and GUIDANCE2 (Supporting Information, Table S7). The reduced dataset included a total of 42 terminals, and the numbers of informative sites were similar to those of the complete dataset before and after the removal of ambiguously aligned positions (Supporting Information, S8–S10).

The best partitioning models of mitochondrial and nuclear genes were estimated independently because their nucleotide composition, substitution rates and among-site rate variation were distinct. The best option was to split *COI* sequences into two blocks (first and second codon positions with a TN+F+I+G4 model, and third codon sites with TN+F+G4), treat rRNA 16S as a single partition with GTR+F+I+G4, and merge nuclear 18S rRNA and 28S rRNA into another partition with TN+F+I+G4. Gene- and site-concordance factors (Minh *et al.*, 2020) were estimated in IQ-TREE v.2.1.3 to assess the number of genes and overall sites supporting each split (node).

Trees built with each of the different alignment approaches, for both complete and reduced datasets,

were compared using approximately unbiased test of phylogenetic tree selection (AU-test; Shimodaira, 2002) as implemented in IQ-TREE v.1.6.12 (Supporting Information S11–S14). This test is generally used to assess topological congruence across markers, but it can also be used to assess congruence between alignments (i.e. whether unreliably aligned positions affect the phylogenetic signal), because alignment, tree topology and branch lengths are inextricably linked in phylogenetic analyses. The best tree and support with 1000 fast bootstrap replicates (-bb 1000, -alrt 0, -abayes) were also estimated under the maximum likelihood criterion in IQ-TREE using ten independent runs. The best partition scheme and best substitution models, based on a reduced set of nucleotide substitution models (-mset JC, F81, K2P, HKY, Tnef, TN, SYM and GTR), were assessed in a preliminary manner in IQ-TREE, using the command -sp TESTMERGE.

Bayesian analyses were run in MrBayes v.3.2.6 (Ronquist & Huelsenbeck, 2003) under the best partitions and models estimated previously in IQ-TREE for 50 million generations sampled every 5000. We set a simpler HKY model instead of TN because the latter is not implemented by default in MrBayes. Six independent analyses were run, and converging runs were combined to ensure that the effective sample size of parameter values was > 200 (sump command in MrBayes) after 50% of burn-in. MrBayes analyses of the full dataset of 78 species did not converge despite running six independent runs of 50 million generations, hence further analyses were discarded. Three of the six independent runs converged after 50 million generations, hence they were combined, and topologies and branch lengths of the sampled trees were summarized after the burn-in in a consensus tree according to their posterior credibility (sumt command in MrBayes).

RESULTS

Phylogeny

The resulting topology from the MAFFT alignment and the complete dataset recovered *Alentia gelatinosa* (M. Sars, 1835) [bootstrap support (BS) 100] and the Eulagiscinae branching off at the base of the ingroup (BS 69; Fig. 2). The other two main clades (Fig. 2A, B, respectively) were recovered gathering the remaining Polynoidae: one containing members of subfamilies Arctonoinae, Lepidastheniinae, Lepidonotinae and Polynoinae (BS 78), and the other including members of Bathyedithinae, Branchinotogluminae, Branchipolynoinae, Lepidonotopodinae, Macellicephalinae, Macellicephaloidinae and Polaruschakovinae (*sensu* Bonifácio & Menot, 2019; BS 79; Fig. 2). Gene and site concordance values supporting the two main clades within Polynoidae were low (one gene and 32% of positions, and two genes and 34% of positions, respectively; Fig. 2). The new species was recovered along with clade A, sister to the clade *Paradyte crinoidicola* (Potts, 1910)–*Gattyana cirrosa* (Pallas, 1766) (BS 65; Fig. 2).

Different alignment methods and removal of poorly aligned positions, divergent regions or taxa did not improve the confidence in placing the new genus *Pollentia* (described below) within the Polynoidae (see trees in Supporting Information S11 and S12). In the reduced dataset, taxa with large amounts of missing data were removed, leaving 42 terminals. In addition, 552 positions were trimmed from the concatenated dataset with Gblocks (153 in 16S rRNA, 109 in 28S rRNA and 290 in 18S rRNA) from the MAFFT *xinsi* alignment. The resulting topology also showed two main polynoid clades containing representatives of the same subfamilies as those obtained using the full dataset (BS 88, zero genes and 45% of positions, and BS 62, three genes and 34% of positions; Fig. 3). The main difference was that now *Pollentia* was recovered as sister to the Eulagiscinae, but still with low support (BS 58, one gene, 33% of sites) and without a conclusive sister-group relationship with other polynoids (Fig. 3). Concordance factors showed an improved support on nodes including *Pollentia*, *Eulagisca gigantea* Monro, 1939 and *Bathymoorea lucasi* Bonifácio & Menot, 2019 in the reduced dataset after removal of unambiguously aligned regions (from zero support for all genes to two out of three genes) because 18S rRNA sequences were missing for *Eulagisca gigantea* and *Bathymoorea lucasi*. The percentage of sites (site-concordance factor) supporting those nodes also increased after trimming from 32.75 and 38.6% to 33.15 to 42.68%, respectively.

The AU-tests of the concatenated analyses showed that the topologies resulting from the different alignment approaches were all congruent except for the GUIDANCE2 alignment including only reliable positions (score 100%; Supporting Information, S13 and S14). In the reduced dataset, AU-tests showed that topologies from the three alignment programs were congruent after excluding ambiguously aligned sites (i.e. GUIDANCE2 alignment with reliable positions only and MAFFT *xinsi* and MUSCLE after Gblocks; Supporting Information, Table S14).

Hence, we selected as the best alignment the reduced dataset comprising 42 taxa and sequences aligned with MAFFT *xinsi* and trimmed with Gblocks. We did so because: (1) this approach improved the phylogenetic signal by removing missing data (e.g. there was an increase of both site- and gene-concordance values); (2) the *xinsi* algorithm took the secondary structure of ribosomal sequences into account (i.e. assigning divergent indels to homologous stem-loop regions); and (3) trimming

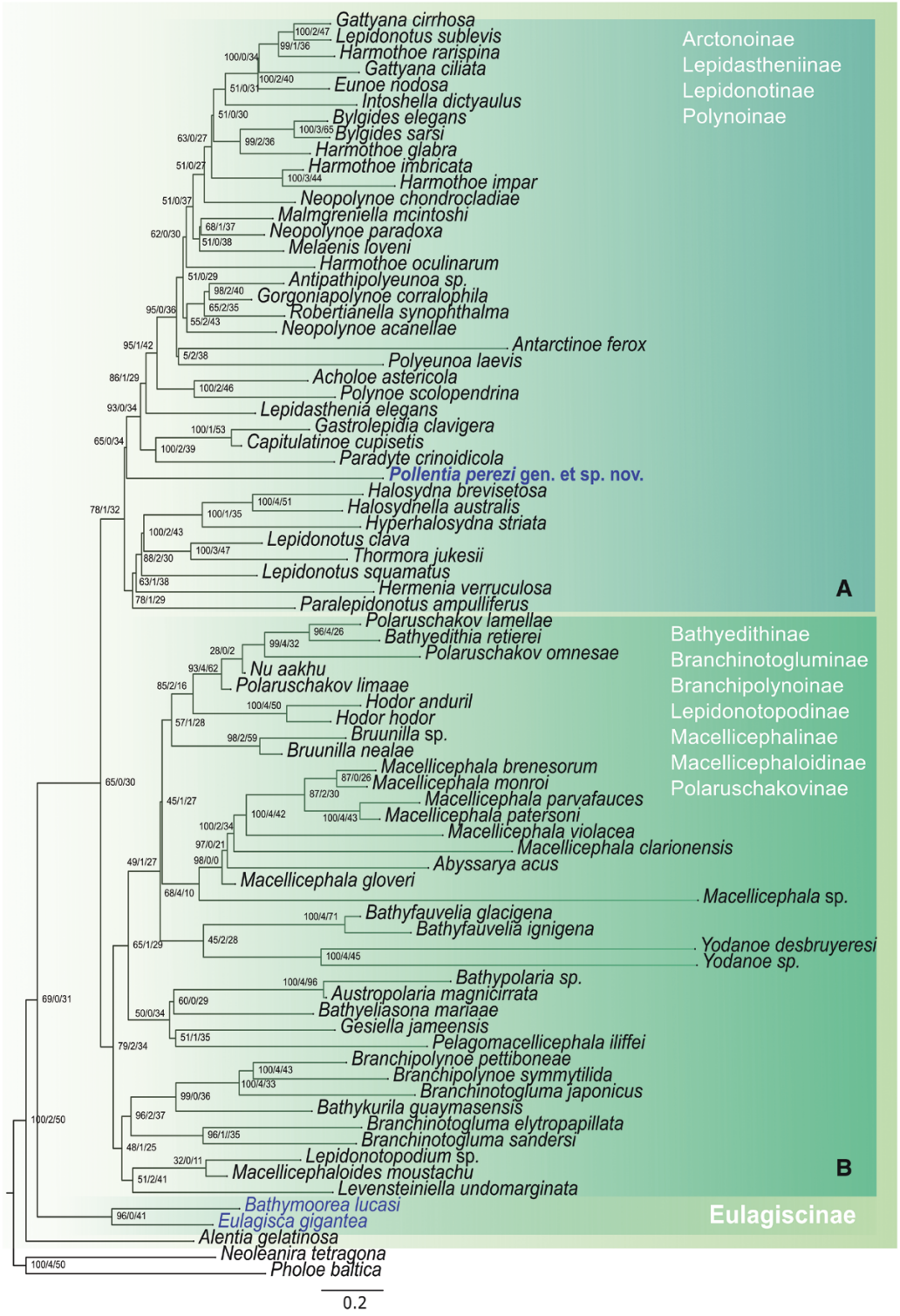

Figure 2. Phylogenetic hypothesis of Polynoidae, yielding two main clades (A, B), inferred from a maximum likelihood analysis based on the full dataset of four concatenated genetic markers (18S rRNA, 28S rRNA, 16S rRNA and *COI*); *COI* was aligned with MUSCLE v.3.8.1551 (Edgar 2004) using default parameters, whereas 18S rRNA, 28S rRNA and 16S rRNA were aligned with MAFFT v.7.397 (Katoh & Standley, 2013) using the *xinsi* option, which considers the secondary structure of RNA. Support values in branches correspond, per order and separated by '/', to the bootstrap support (BS) values of the maximum likelihood IQ-TREE, the number of genes (concordance) and the number of positions (concondance).

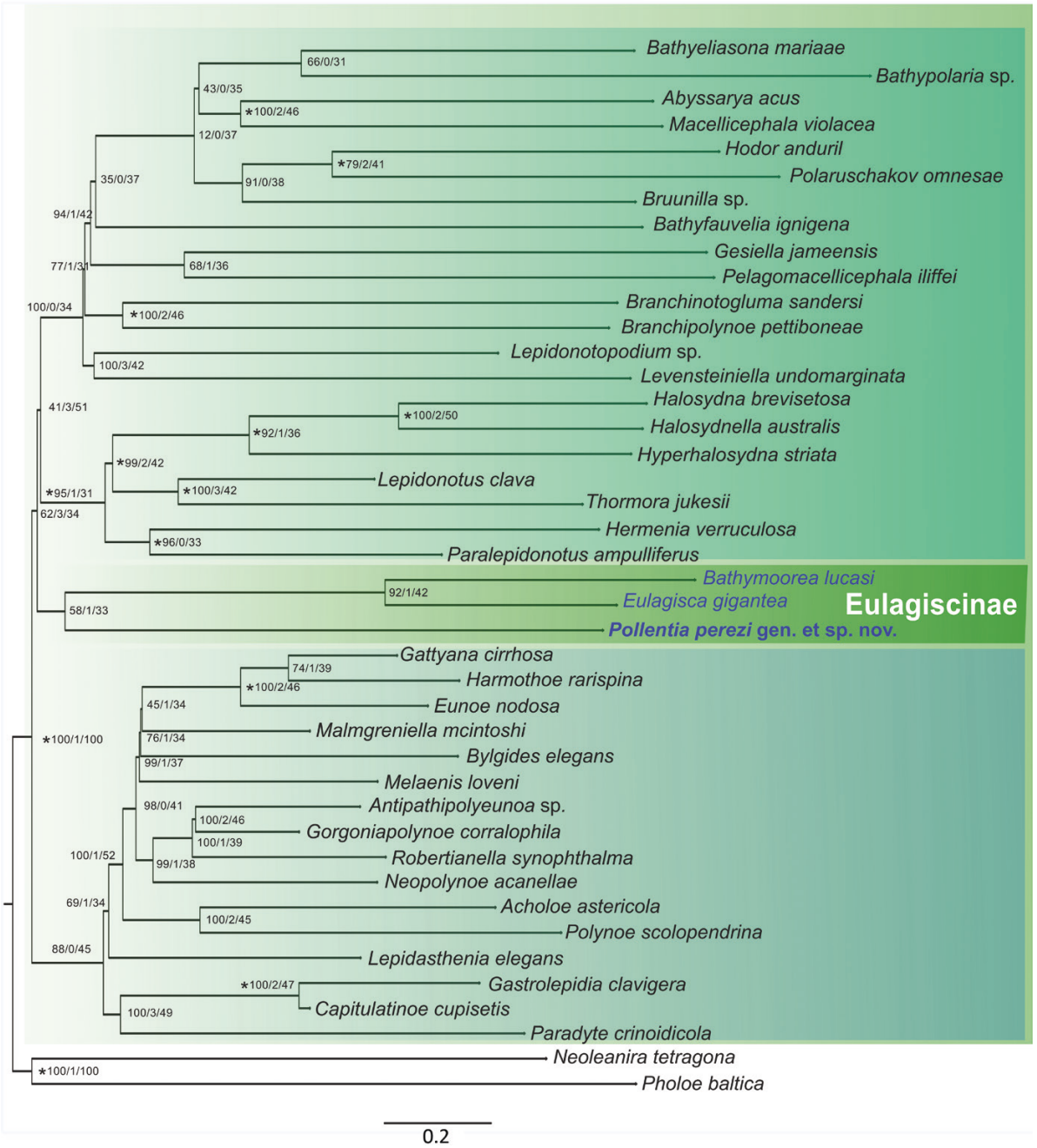

Figure 3. Phylogenetic hypothesis of Polynoidae inferred from a maximum likelihood analysis based on the reduced dataset of four concatenated genetic markers (18S rRNA, 28S rRNA, 16S rRNA and *COI*). Alignment was performed with MUSCLE for *COI*, using default parameters, and with MAFFT for 18S rRNA, 28S rRNA and 16S rRNA, using the *xinsi* option. Ambiguously aligned positions were removed with GBLOCKS. Support values in branches correspond, per order and separated by '/', to the bootstrap support (BS) values of the maximum likelihood IQ-TREE, the number of genes (concordance) and the numbers of positions (concordance). *Posterior probabilities > 0.9 recovered after Bayesian inference in MRBAYES.

removed unreliably aligned positions (i.e. non-homologous residues despite being placed in the same position). Maximum likelihood and Bayesian analyses of the reduced dataset of 42 taxa based on MAFFT *xinsi* alignments trimmed in GBLOCKS retrieved similar tree topologies, except for a few nodes (Fig. 3). MRBAYES did not recover Eulagistinae as monophyletic. However, the new taxon, *Pollentia*

perezi, was recovered with low support as sister to *Eulagisca gigantea* (posterior probability of 0.33).

SYSTEMATICS

ANNELIDA LAMARCK, 1802

APHRODITIFORMIA LEVINSEN, 1883

POLYNOIDAE KINBERG, 1856

EULAGISCINAE PETTIBONE, 1997

Eulagiscinae Pettibone, 1997: 537–538; Bonifácio & Menot 2019: 573.

Amended diagnosis: Body elongate, with ≤ 41 segments. Prostomium bilobed. Two pairs of eyes present (*Eulagisca* McIntosh, 1885 and *Pareulagisca* Pettibone, 1997) or eyes absent (*Pollentia* and, presumably, *Bathymoorea* Pettibone, 1967). Median and lateral antennae present; lateral antennae inserted terminally or subterminally on anterior extension of prostomium. Facial tubercles absent (*Pareulagisca* and *Pollentia*) or present (*Eulagisca* and *Bathymoorea*). Tentaculophores provided with acicula and chaetae (*Eulagisca*, *Bathymoorea lucasi* and *Pollentia*), without acicula and with chaetae (*Pareulagisca*) or achaetous [*Bathymoorea renotubulata* (Moore, 1910)]. Nuchal fold absent (*Bathymoorea* and *Pollentia*) or present (*Eulagisca* and *Pareulagisca*). Pharynx with two pairs of jaws. Dorsal tubercles present. Elytrophores bulbous, ≤ 16 pairs, on segments 2, 4, 5, 7, 9, 11, 13, 15, 17, 19, 21, 23, 26, 29, 32 and 33. Parapodia subbiramous, notopodia shorter than neuropodia; noto- and neuropodia provided with elongate acicular lobe; tips of noto- and neuroaciculae not penetrating epidermis. Notochaetae numerous, with spinous rows; neurochaetae numerous.

Remarks: The Mallorcan cave polynoid described herein as *Pollentia* shows features considered to be diagnostic of members of Eulagiscinae: the simple lateral antennae (without distinct ceratophores) are inserted terminally or subterminally on anterior extensions of the prostomium, a character also shared with members of Lepidastheniinae and Lepidonotinae but not present in Harmothoinae, whose members have lateral antennae inserted ventrally and with distinct ceratophores (Pettibone, 1997; Bonifácio & Menot, 2019). Parapodia have prominent conical and thin acicular lobes and numerous noto- and neurochaetae in *Pollentia* and other members of Eulagiscinae; but notopodia are less prominent than notopodia and therefore considered as subbiramous. These parapodia are distinguished from the vestigial or poorly developed notopodia found in members of Lepidonotinae and Lepidastheniinae (Wehe, 2006). The Mallorcan cave polynoids described herein show some morphological features, such as the number and arrangement of elytra and chaetal morphology (described in detail below), that have not been reported previously among members of Eulagiscinae.

Until the present study, Eulagiscinae consisted of eight species (Table 4). The subfamily diagnosis was recently amended by Bonifácio & Menot (2019), but it requires further modification in order to accommodate the morphological disparity observed in *Pollentia* and other members of the subfamily. Thus, the number of pairs of elytra in *Pollentia* (13 pairs) is the lowest reported in the subfamily, because members of *Eulagisca* bear 15 pairs, *Paraeulagisca* 16 pairs and *Bathymoorea* 14 pairs (Table 5; Pettibone, 1967, 1997; Bonifácio & Menot, 2019). Members of Eulagiscinae are reported to have eyes: two pairs occur in *Eulagisca* and *Pareulagisca*, whereas one pair of presumed large eyes was described in *Bathymoorea* (Bonifácio & Menot, 2019). However, the large coloured brain (C. Helm, pers. comm.) of *Pollentia*, visible through the translucent integument (Figs 4, 5A–C), could correspond to the structure interpreted as 'large opaque ocular areas' in *Bathymoorea renotubulata* (Pettibone, 1967) or the 'large eyes' described in *Bathymoorea lucasi* (Bonifácio & Menot, 2019). Members of *Paraeulagisca* display two types of notochaetae (Pettibone, 1997), whereas there is only one type in *Bathymoorea*, *Eulagisca* (Bonifácio & Menot, 2019) and in *Pollentia*.

POLLENTIA GEN. NOV.

Zoobank registration: urn:lsid:zoobank.org:act:A0CCEE32-94FE-44C7-BB1D-C4DD85D58FB5

Diagnosis: Body flattened dorsoventrally, with ≤ 27 segments (Fig. 4). Prostomium bilobed (Fig. 5A–C). Frontal filaments absent. Eyes absent (Fig. 5A–C). Median and lateral antennae present; lateral antennae inserted subterminally on extensions of prostomium (Fig. 5A–C). Facial tubercle absent. Tentaculophores with acicula and chaetae (Figs 5, 6B). Dorsal tubercles present. Elytrophores large, 13 pairs: one pair on each of segments 2, 4, 5, 7, 9, 11, 13, 15, 17, 19, 21, 23 and 26. Elytra large, covering dorsum, lacking papillae, each with microtubercles along external edge and posterior dorsal surface. Parapodia subbiramous; noto- and neuropodia with elongate acicular lobe. Notochaetae with spinous rows and pointed tips. Neurochaetae numerous, of two types: superior, flattened, with spinous rows and with tridentate tip; and inferior, shorter and thinner, lanceolate and pectinate, with

Table 4. Current valid nominal species of Eulagiscinae, including type locality, coordinates, depth and reported distribution

Species	Type locality	Coordinates	Depth	Reported distribution
Bathymoorea lucasi Bonifácio & Menot, 2019	Clipperton Fracture Zone, East Pacific	18°48′N, 128°19′W	4933 m	Clarion-Clipperton Fracture Zone, 4933–4964 m (Bonifácio & Menot, 2019)
Bathymoorea renotubulata (Moore, 1910)	Santa Catalina Island, California	33°43′N, 117°42′W	4016 m	Off southern California, 4016–4074 m
Eulagisca corrientis McIntosh, 1885	Off Buenos Aires, Argentina	37°17′S, 53°52′W	1097 m	South Atlantic and South Indian Oceans, 274–1097 m (Pettibone, 1997)
Eulagisca gigantea Monro, 1939	Off Princess Elizabeth Land, Antarctic	6°48′S, 71°24′E	540 m	Antarctic, off Princess Elizabeth Land, Davis Sea, Drake Passage, Scotia Sea, South Shetlands, South Orkneys, 200–900 m (Pettibone, 1997)
Eulagisca macnabi Pettibone, 1997	Off South Orkney Island Antarctic	61°00′S, 44°58′W	283 m	Antarctic, South Orkneys, 300 m (Pettibone, 1997)
Eulagisca puschkini Averincev, 1972	Davis Sea, Antarctic	–	32 m	Antarctic, Davis Sea, 12 m (Pettibone, 1997)
Eulagisca uschakovi Pettibone, 1997	Off MacRobertson Land, Antarctic	66°45′S, 62°63′E,	219 m	Antarctic, off MacRobertson Land, off Enderby Land, Davis Sea, Bransfield Strait, off Palmer Archipelago, Scotia Sea, Elephant Island, South Orkneys, Ross Sea, Weddell Sea, in 10–920 m
Paraeulagisca panamensis (Hartman, 1939)	Piñas Bay, Panama	07°34′N, 78°12′W	Intertidal	Central Pacific Ocean, Panama, intertidal (Pettibone, 1997)

spinous rows and tapering. Nephridial papillae present from segment 5 onwards.

Remarks: The erection of a new genus is required to accommodate this taxon because it shows some unique features not reported in any other member of the subfamily Eulagiscinae, namely, the display of 13 pairs of elytra and the morphology and arrangement of noto- and neurochaetae. In addition, *Pollentia* shows a unique combination of features: eyelessness; tentaculophores bearing acicula and chaetae; nephridial papillae present from segment 5 onwards; only one type of notochaetae present from segment 2 onwards, stout and spinous; and two types of neurochaetae: superior flattened, spinous and tridentate; and inferior smaller, lanceolate and pectinate with spinous rows reaching the tip.

Etymology: Generic name refers to *Pollentia*, an ancient Roman city located in the current Mallorcan municipality of Alcúdia, where the cave harbouring the new taxon is located. Gender feminine.

Type species: Pollentia perezi sp. nov., described herein, by monotypy.

POLLENTIA PEREZI SP. NOV.

(FIGS 3, 4, 5, 6)

Zoobank registration: urn:lsid:zoobank.org:act:DF4ED4DA-818A-49E0-9996-AFDB2FAD73FA

Type material: Cova des Bastons (also known as Cave C-11), Alcúdia, Mallorca, Balearic Islands, 39°53′03.1″N, 3°11′45.1″E. **Holotype**: specimen preserved in ethanol; collected by J. Pérez at 17 m depth on bare rock with some patches of calcareous silt, 11 March 2020 (*MNCN 16.01/18955*) (Supporting Information Video S15). **Paratype**: specimen preserved in ethanol, divided into two fragments, same collector, locality, substratum and depth, 30 June 2019 (MNCN 16.01/18956).

Additional material examined: specimen preserved in RNAlater, same collector, locality, substratum and depth as holotype (deposited at IMEDEA collection) (see Supporting Information Video S16).

Description of holotype: Body length 18 mm, maximum width 6 mm at midbody segments (including parapodia;

Table 5. Main morphological diagnostic features of members of Eulagiscinae

Feature	*Eulagisca*	*Paraelagisca*	*Bathymoorea*	*Pollentia* gen. nov.
Visibly pigmented brain	Absent	Absent	Present	Present
Eyes	Two pairs	Two pairs	Absent?*	Absent
Facial tubercles	Present	Absent	Present	Absent
Tentaculophore acicula	Present	Absent	Absent/present	Present
Tentaculophore chaetae	Present	Present	Absent/present	Present
Nuchal fold	Present	Present	Absent	Absent
Elytrophores/elytra	15	16	13	13
Dorsal tubercles	Bulbous/nodular	Bulbous/nodular	Lamelliform/inflated	Inconspicuous
Notochaetae	One type: stout and spinous	Two types: stout, smooth or spinous and slender capillary	One type: either stout and spinous or fine spines	One type: stout and spinous
Neurochaetae	One type: tapering, spinous with slender, bare, pointed tips	One type: tapering, spinous, with bare pointed tip and minute secondary tooth	One type: long, distally flattened, spinous and pointed tip	Two types: flattened, spinous and tridentate, and lanceolate, spinous and tapering tip

*A pair of large eyes was described in *Bathymoorea renotubulata* by Pettibone (1967) and in *Bathymoorea lucasi* by Bonifácio & Menot (2019), but these are considered herein as potential misinterpretations.

excluding chaetae). Body 27-segmented, flattened dorsoventrally, anterior margin blunt, tapering posteriorly (Fig. 4). Specimen pale when alive, with some tiny brown spots scattered over dorsum, forming narrow segmental transverse bands near base of notopodia and elytrophores, and on ventrum near base of parapodia (Figs 4, 5C, D). Head intensely coloured dark red (pigmented brain visible through translucent epithelium; Figs 4A, C, D, 5A–C).

Prostomium bilobed, wider than long, with lobes extending anteriorly to form ceratophores of lateral antennae (Figs 5A–C, 6A). Median antenna inserted proximal to anterior margin of prostomium; ceratophore bulbous, longer than wide (Figs 5B, 6A); style tapering, reaching segment 3 (Fig. 5B). Lateral antennae with styles also tapering, shorter than median antenna (Fig. 5A, B). Median and lateral antennae with scattered long papillae on styles (Fig. 6A–C). Palps stout and longer than antennae, reaching segment 6, heavily wrinkled and covered with minute oval papillae (Figs 4D, 5A, 6B, E, F). Eyes absent (Figs 4A, C, D, 5A–C).

Tentacular segment (segment 1) with short lobe inserted lateral to prostomium; aciculae not penetrating epidermis; bundle of about six notochaetae (Figs 5A, C, 6B, H). One pair of tentacular cirri present on each side of segment; tentaculophores longer than wide, ventral larger than dorsal (Fig. 6H); tentacular styles tapering, dorsal and ventral of similar length, reaching segment 5 (Fig. 4D); styles covered with elongated papillae (Fig. 6I). Mouth lips strongly developed, protruding when pharynx not everted (Fig. 5E). Facial tubercle absent, but slightly inflated longitudinal ridge present on upper lip (Fig. 6B, G). Pharynx not everted in holotype and dissected in paratype, with ring of elongate, blunt subconical papillae of similar size (Fig. 6M, not counted) and two pairs of jaws with smooth margins (Fig. 6N). Segment 2 devoid of nuchal pads and folds (Fig. 6A–C).

Thirteen pairs of elytra, one on each of segments 2, 4, 5, 7, 9, 11, 13, 15, 17, 19, 21, 23 and 26. Elytra large, covering dorsum, lacking papillae, each with microtubercles along external edge (Fig. 7A–D) and on dorsal surface of posterior third (Fig. 7E). Surface of anterior part of elytra smooth (Fig. 7F). Dorsal cirri present on non-elytrigerous segments from segment 3 onwards; cirrophores cylindrical (Fig. 8A–C); styles elongated and tapering, largely surpassing length of parapodia and chaetae, of similar length (Figs 4C, D, 8F, H), with some long, scattered papillae. Dorsal tubercles inconspicuous, low and conical, more evident on elytrigerous segments (Fig. 8B).

Segment 2 with subbirramous parapodia, enlarged conical acicular lobe, and noto- and neurochaetae (Fig. 6H). Ventral cirri of segment 2 (buccal cirri) inserted

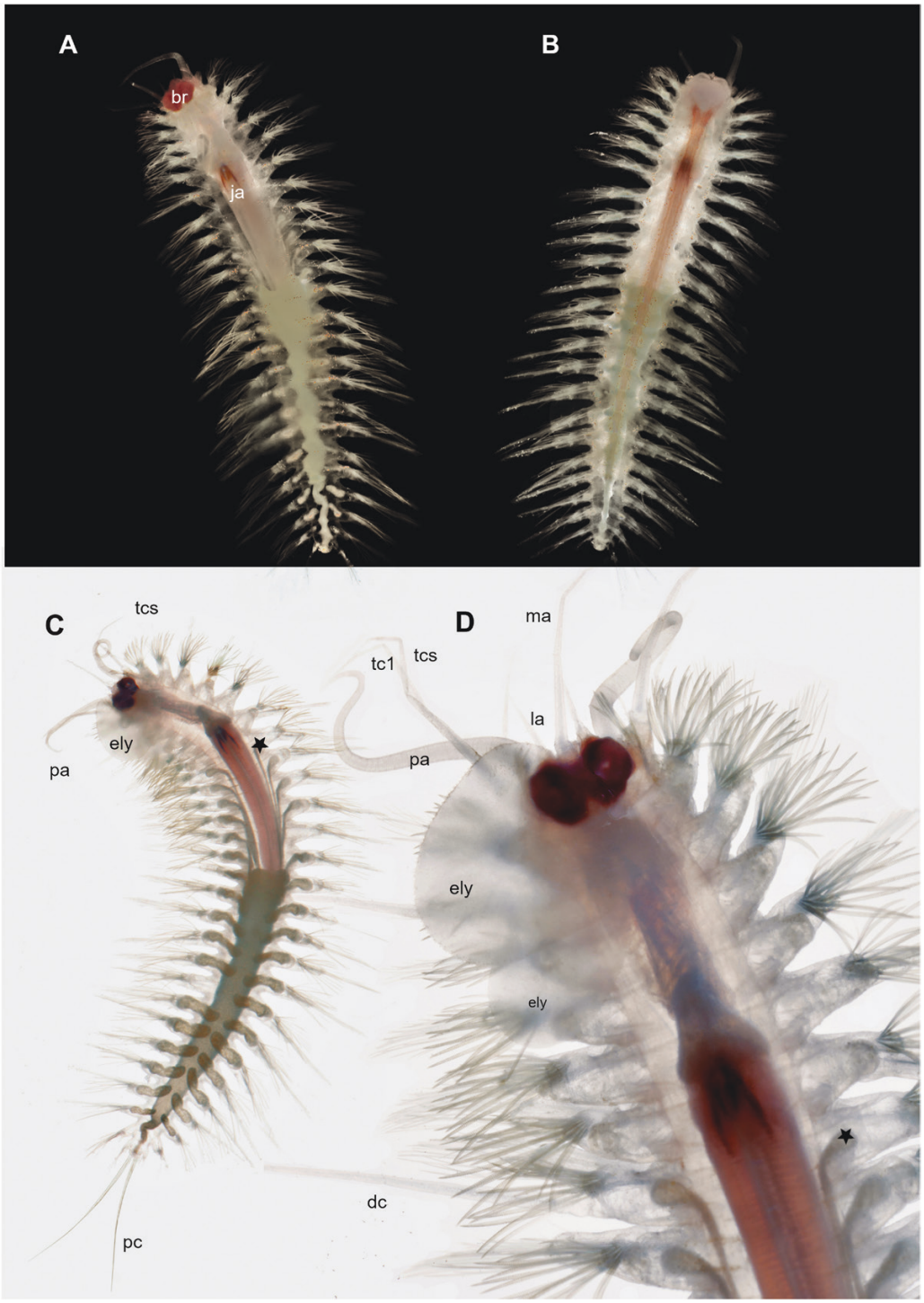

Figure 4. *Pollentia perezi* gen. & sp. nov. live specimen. A, dorsal view, showing spotted pigmentation pattern, holotype *MNCN 16.01/18955*. B, ventral view, showing spotted pigmentation pattern, holotype *MNCN 16.01/18955*. C, dorsal view, paratype MNCN 16.01/18956. D, detail of anterior end; notice two elytra still attached on first two left elytrophores, paratype MNCN 16.01/18956. Images courtesy of WhiteLife Photography. Abbreviations: br, brain; cma, ceratophore median antenna; dc, dorsal cirrus; ely, elytra; ja, jaws; la, lateral antenna; li, lip; ma, median antenna; np, nephridial papillae; pa, palp; tc1, inferior tentacular cirrus; tcs, superior tentacular cirrus; stars, nephridial ducts.

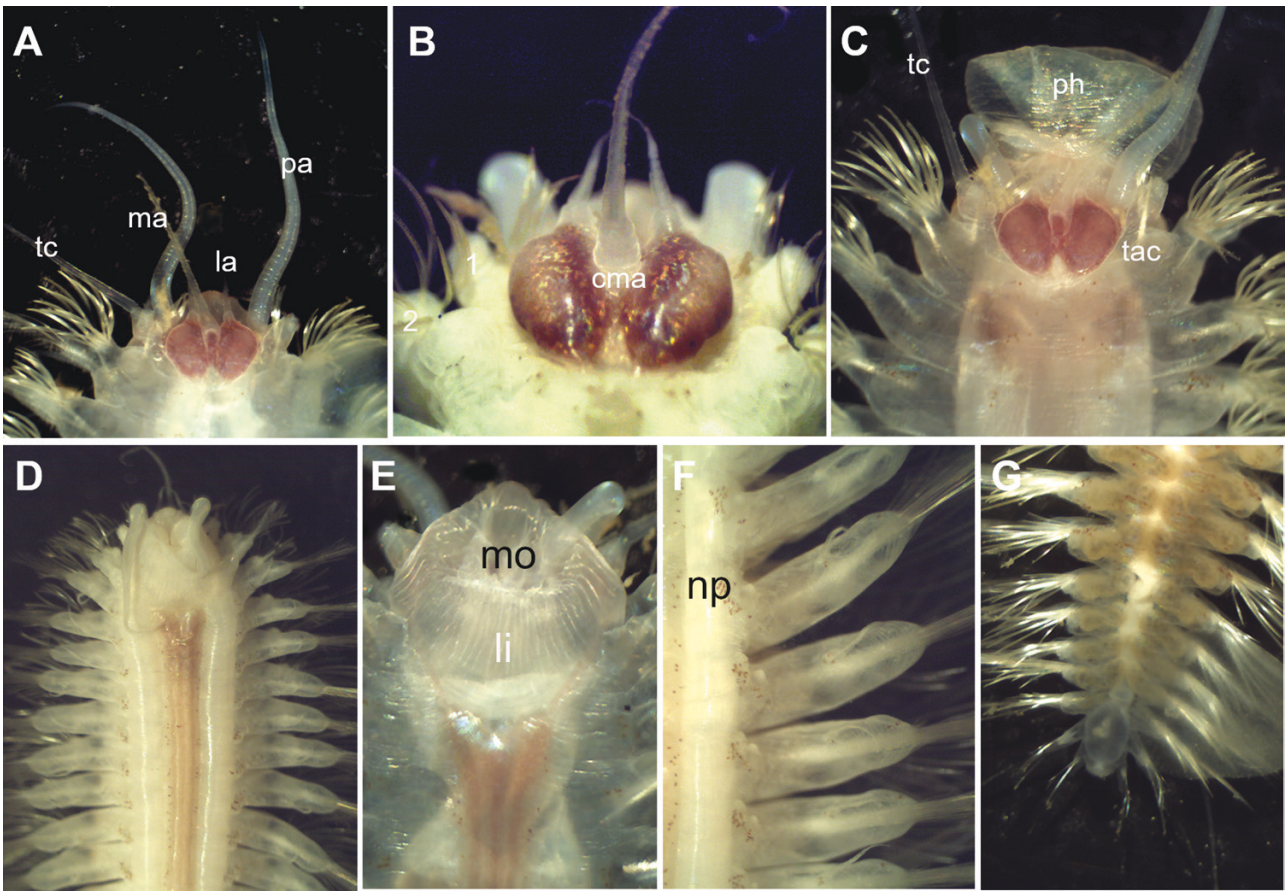

Figure 5. *Pollentia perezi* gen. & sp. nov. (holotype *MNCN 16.01/18955*) specimen, with all elytra accidentally lost except for a posterior one. A, anterior segments, dorsal view, live specimen. B, detail of prostomium and head appendages, preserved specimen. C, anterior segments of live specimen, with proboscis partly everted. D, anterior segments, ventral view, preserved specimen. E, detail of anterior margin, showing mouth. F, anterior parapodia, ventral view, showing nephridial papillae. G, posterior segments, dorsal view. Abbreviations: cma, ceratophore median antenna; la, lateral antenna; li, lip; ma, median antenna; mo, mouth; np, nephridial papilla; pa, palp; ph, pharyx; tc, tentacular cirrus.

basally, with large cirrophores; stylode longer than subsequent counterparts, with elongated papillae (Fig. 6I). Rest of segments also with subbiramous parapodia and with thin and long, tapering acicular lobes projecting on both rami; notoacicular lobe shorter than neuroacicular and hidden under the inferior notochaetae (Fig. 8B); neuroacicular lobe conspicuous (Fig. 8E, G); noto- and neuroaciculae not penetrating into lobes (Fig. 8D, E, G). Notopodia rounded, one-third the length of neuropodium; latter subconical, with further indistinct lobes other than the acicular projections (Fig. 8E–G). Ventral cirri inserted at midlength of neuropodia (Fig. 8E–G), with short ceratophore and smooth, tapering style reaching about midlength of parapodia (Fig. 8A, B). Styles of ventral cirri of segments 2 and 3 longer than subsequent counterparts, with elongated papillae (Fig. 8H–K); styles from segment 4 onwards all similar in length, without papillae (Fig. 8I, L). Semispherical papillae ventrally at base of parapodia (Fig. 8M).

Notochaetae of all segments similar, of only one type (~20 on parapodia of anterior and midbody segments), stouter than neurochaetae, arranged in dense, radiating tufts (Fig. 9A, B). Notochaetae smooth and straight basally, slightly curved and tapering, with well-developed spinous rows along convex margin (Fig. 9A-C) and pointed, conical tips. Two types of neurochaetae (30–40 on parapodia of midbody segments) arranged in transverse rows. Superior neurochaetae flattened, with one side bearing faintly spinous rows (Fig. 9D-F); tip tridentate, with a slightly hooked tooth and two additional smaller teeth (Fig. 9F). Inferior neurochaetae shorter and thinner than superior counterparts, each with a cylindrical proximal half and a broader, lanceolate and flattened distal half; one of sides with well-developed spinous rows reaching the tip (Fig. 9G, H).

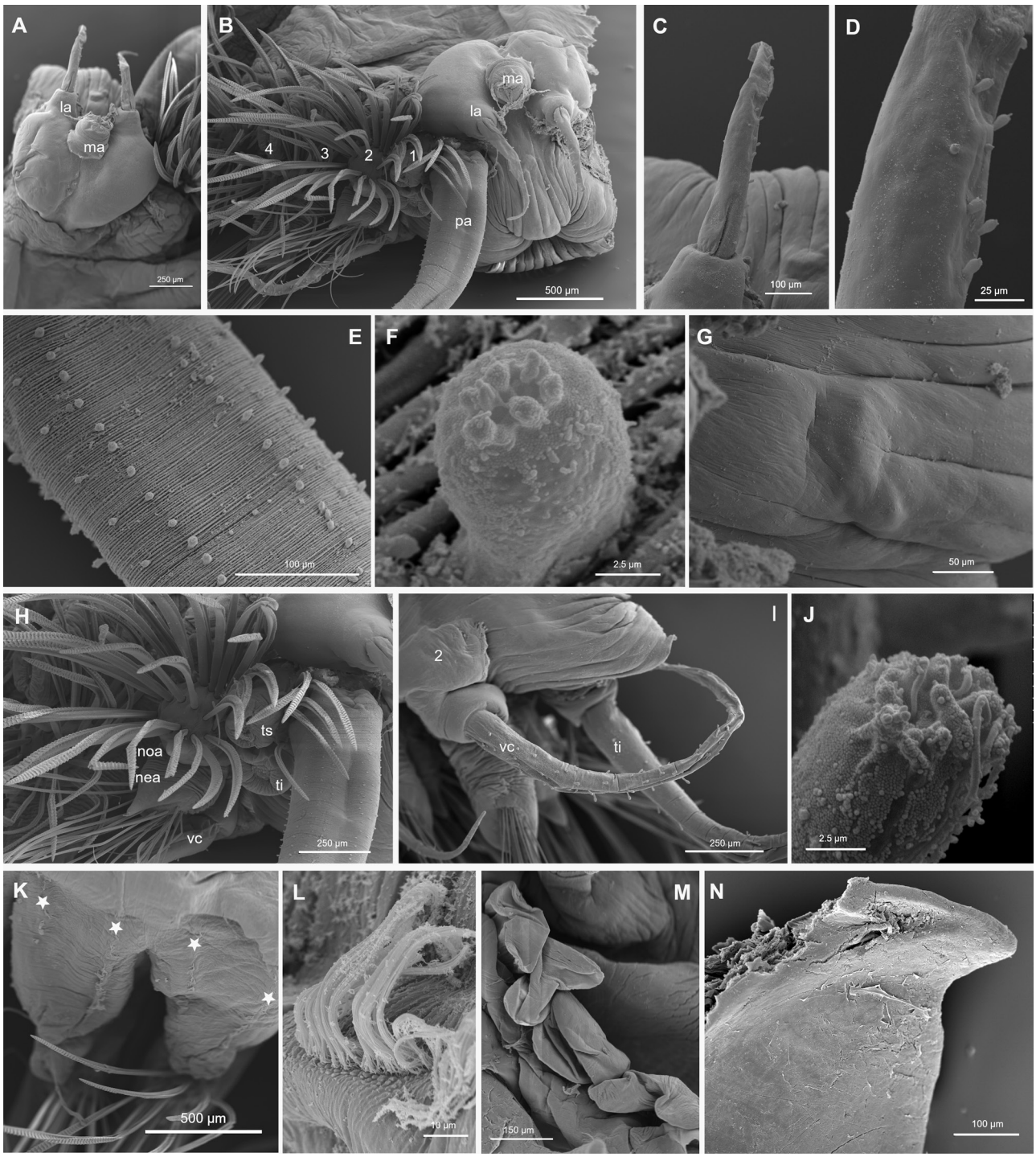

Figure 6. *Pollentia perezi* gen. & sp. nov. (paratype MNCN 16.01/18956). A, head with dissected appendages except for lateral antennae. B, head and anterior parapodia, side view (tentacular cirri with removed styles). C, lateral antenna. D, detail of lateral antenna, with internal papillae. E, detail of wrinkled palp, with longitudinal rows of papillae. F, papilla on palp. G, upper lip, without facial tubercle. H, second segment, with wide neuropodial acicular lobe. I, ventral cirrus of second segment. J, detail of papilla of first ventral cirrus. K, transverse rows of cilia on midbody dorsal sides. L, detail of dorsal rows of cilia. M, pharyngeal papillae. N, detail of jaw. Abbreviations: la, lateral antenna; ma, median antenna; mo, mouth; nea, neuroacicular lobe; noa, notoacicular lobe; pa, palp; ph, pharyx; tc, tentacular cirrus; ti, inferior tentacular cirrus; ts, superior tentacular cirrus; vc, ventral cirrus; 1–4, segment number; stars, rows of cilia.

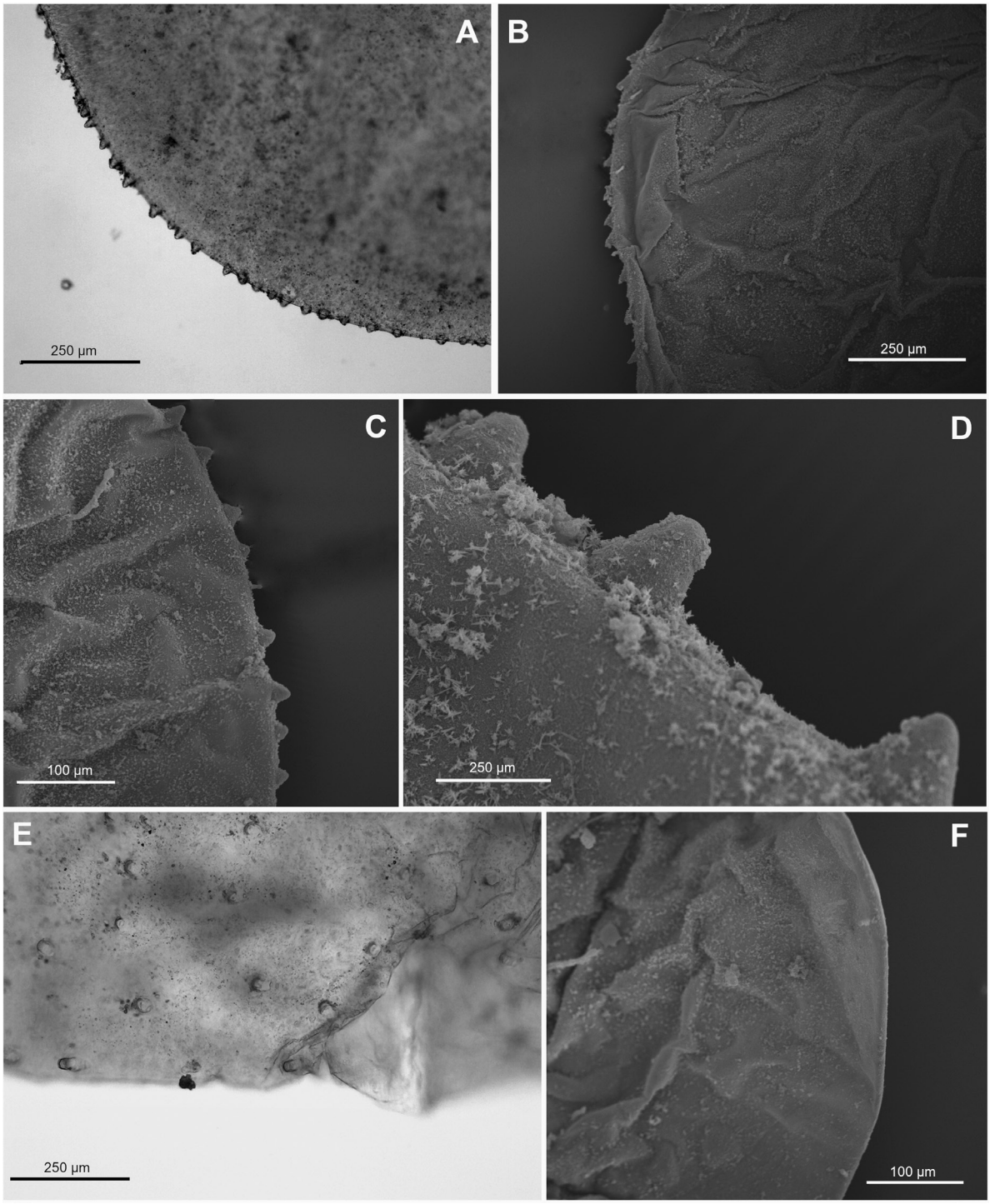

Figure 7. *Pollentia perezi* gen. & sp. nov. (paratype MNCN 16.01/18956), elytra. A, outer edge, with microtubercles. B, same, scanning electron micrograph. C, D, detail of microtubercles, scanning electron micrograph. E, light micrograph of tubercles on outer surface. F, smooth inner edge, scanning electron micrograph.

Unpigmented nephridial papillae present at base of parapodia from segment 5 onwards, small and bulbous. Nephridial papillae from segment 8 onwards connect to posterior half of body through long ducts, visible under light microscopy. Pygidium small, rounded, not enclosed by last segment (Fig. 5G), with anus placed terminally. Pair of anal cirri longer than dorsal cirri.

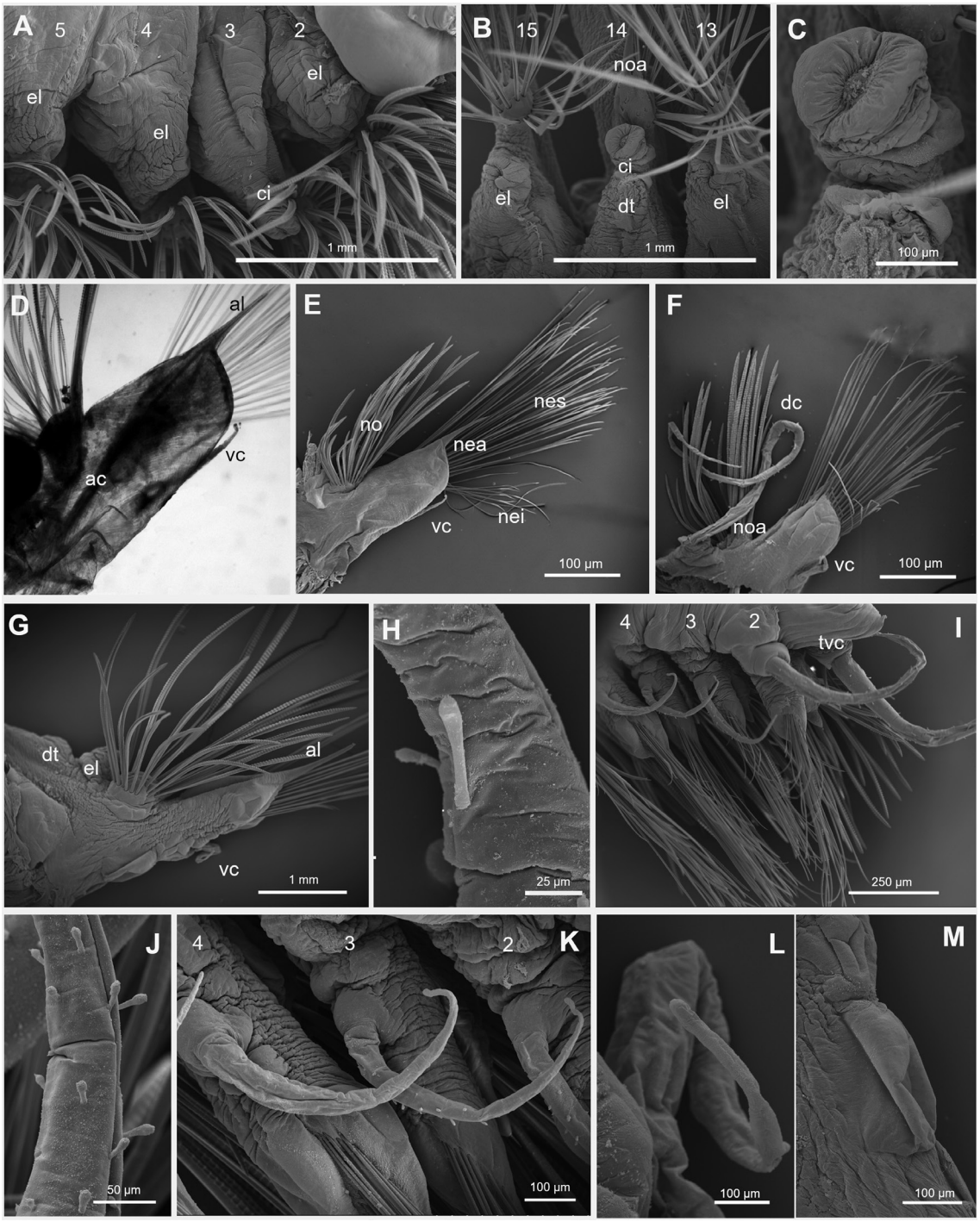

Figure 8. *Pollentia perezi* gen. & sp. nov. (paratype MNCN 16.01/18956), parapodia. A, anterior parapodia, showing arrangement of elytrophores and cirrophores. B, dorsal view of parapodia of segments 13–15. C, detail of cirrophores, segment 14. D, micrograph of midbody parapodium, anterior view, showing neuroacicula by transparency. E, midbody parapodium, anterior view, scanning electron micrograph, showing chaetal bundles and tapering neuroacicular lobe. F, scanning electron micrograph of midbody parapodium with dorsal cirrus, posterior view. G, midbody parapodium ventral view, with elytrophore and a low, inconspicuous dorsal tubercle. H, detail of papilla on dorsal cirrus. I, anterior parapodia, ventral view. J, detail of papillae ventral cirrus segment 3. K, ventral cirri, smooth from segment 4. L, midbody ventral cirrus. M, ventral papilla. Abbreviations: al, acicular lobe; ci, cirrophore; dc, dorsal cirrus; el, elytrophore; nea, neuroacicular lobe; nei, interior neurochaetae; nes, superior neurochaetae; no, notochaetae; noa, notoacicular lobe; vc, ventral cirrus; 1–15, segment number.

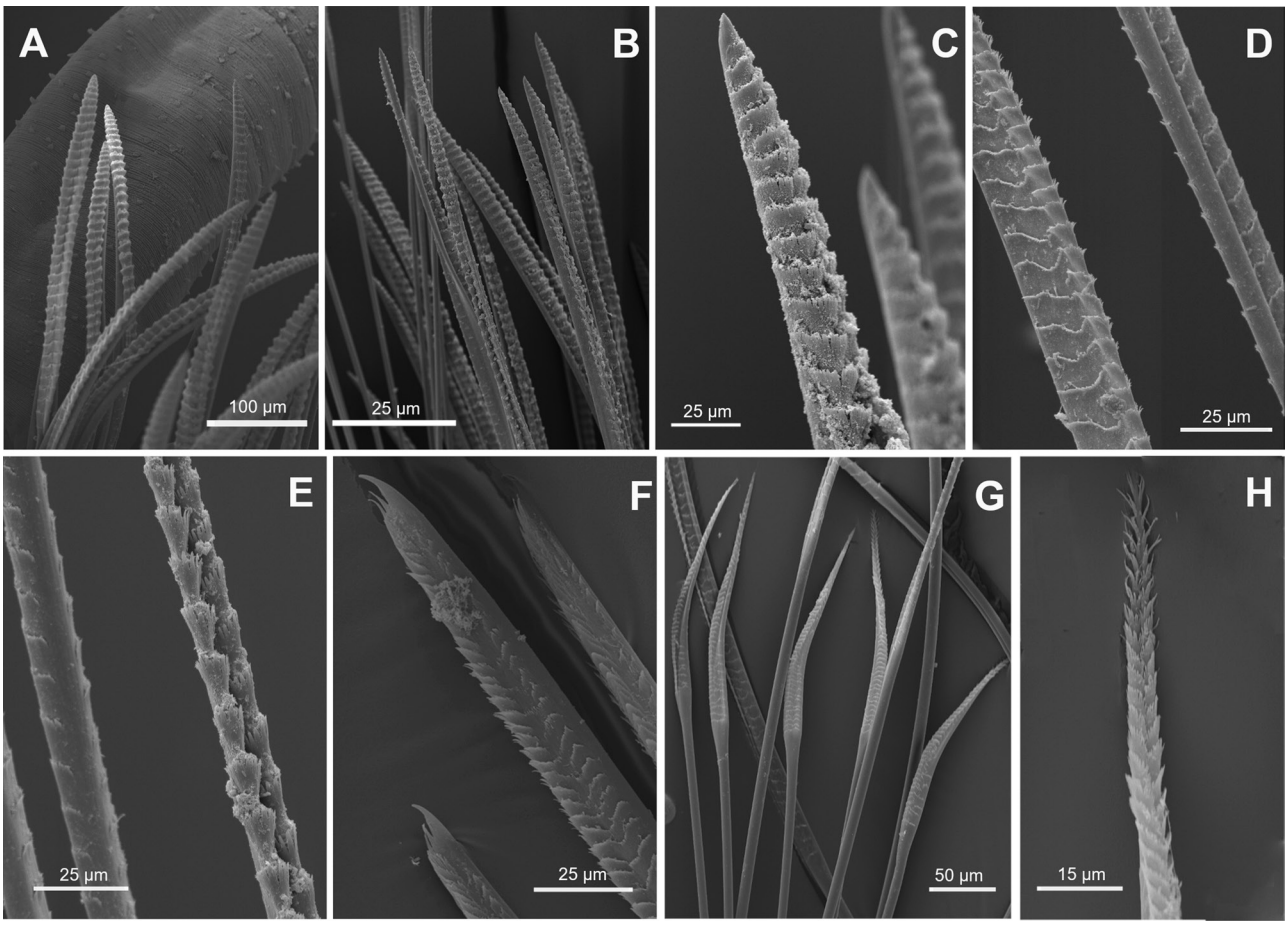

Figure 9. *Pollentia perezi* gen. & sp. nov. (paratype MNCN 16.01/18956), chaetae. A, notochaetae tentacular segment (segment 1). B, notochaetae bundle. C, detail of tip of notochaetae. D, E, detail of superior neurochaetae, mid length. F, detail of distal end of superior neurochaetae. G, inferior neurochaetae. H, detail of distal end of inferior neurochaeta.

Intraspecific variability: Paratype, with 26 segments, measuring 18 mm long (including tentacular segment) and maximum width 6 mm at midbody segments (including parapodia; excluding chaetae). Pigmentation pattern similar to holotype (Figs 4, 5). Specimen with most elytra detached after preservation. Most other morphological features as for holotype (Figs 4, 5).

Ecology: The first specimen was found and collected after scuba divers accidentally dropped an object on the sandy bottom of the cave and the animal escaped from danger, ascending to the water column (Supporting Information Videos S15, S16). The other two specimens were each found in subsequent visits to the cave, crawling on the sediment. In all cases, specimens were found at 17 m depth in full-strength marine water (38 PSU) at 19 °C (Fig. 1C).

Etymology: Species named after the Mallorcan cave diver Joan Pérez, who discovered the species and kindly offered the material to us for study.

Remarks: The new Mallorcan cave polynoid bears an overall resemblance to members of the subfamily Eulagiscinae, in that they all share the terminal or subterminal insertion of the lateral antennae on anterior extensions of the prostomium, and the parapodia display notopodia shorter than neuropodia, unlike members of other related subfamilies (Wehe, 2006; Bonifácio & Menot, 2019). However, there are some morphological features that are unique among the current members of Eulagiscinae. The number of pairs of elytra, 13 in *Pollentia perezi*, is the lowest reported in the subfamily (Table 5; Pettibone, 1967, 1997; Bonifácio & Menot, 2019). In addition, the chaetal morphology and arrangement in *Pollentia perezi* are unique amongst members of Eulagiscinae and even Polynoidae. Thus, body segments from segment 2 onwards bear only stout notochaetae with spinous rows and pointed tips, similar to those described in *Eulagisca* and *Bathymoorea lucasi* (Table 5). Neurochaetae are of two types: the superior flattened, spinous and with a tridentate tip, whereas

the inferior are shorter and thinner, lanceolate, spinous and tapering (Table 5). Furthermore, the superior neurochaetae are unique amongst those of Polynoidae, because they have a tridentate tip, with a main larger tooth and two additional smaller teeth. The inferior neurochaetae resemble the pectinate forms described in members of Eulepethidae (Pettibone, 1969).

Both *Eulagisca* and *Paraeulagisca* are oculate (each bearing two pairs of eyes). The two nominal species of deep-sea *Bathymoorea* were described as bearing a pair of large eyes, but we consider this to be a misinterpretation of the brain occupying most of the prostomial lobes, as in the anchialine *Pollentia perezi*, which is eyeless. Like its deep-sea relatives, *Pollentia perezi* lacks body pigmentation except for a few scattered spots distributed as described above.

DISCUSSION

The new taxon described herein belongs to a subfamily (Eulagiscinae) whose known members were thought to be mostly limited to cold marine waters (Table 4), whether in the deep sea at low latitudes (i.e. *Bathymoorea*, in the western Pacific seafloor at 4000–5000 m depth; Moore, 1910; Pettibone, 1967; Moore, 2010) or in shallower environments at higher latitudes (i.e. species of *Eulagisca*, occurring in the Antarctic Ocean and South America at depths of 30–1100 m; Pettibone, 1997). Such cases of so-called 'isothermic submersion', involving populations that have become separated long enough to become distinct at the species or generic level, are well known among marine zoogeographers (Briggs, 1995). Only the monotypic *Pareulagisca panamensis* (Hartman, 1939), described from the littoral zone of the Panamanian Pacific, is an apparent exception to this rule among eulagiscins. However, the phylogenetic position of this taxon has never been assessed through molecular analyses, whereas its morphology (e.g. display of two different types of notochaetae, different number and morphology of elytra and lack of facial tubercles, among other features) suggests that it might perhaps not be closely related to Eulagiscinae.

Racovitza (1907) was first to link the eventual presence of deep-sea forms in marine caves to the concurrence of exceptional circumstances in which cave water temperature remains anomalously low. He rejected previous assumptions made by Fuchs (1894) on the primary adaptation of the inhabitants of the deep sea to permanent darkness rather than to a permanently cold environment, and on their consequent propensity to colonize marine caves. Racovitza remarked that, if the assertions of Fuchs were right, many of the marine cave dwellers should be deep-water instead of littoral forms, which they are not. Indeed, Racovitza's (1907) hypothesis is strongly reinforced by findings such as the recent records of the presumed Mediterranean endemic stygobiont carnivorous sponge *Asbestopluma hypogea* Vacelet & Boury-Esnault, 1996 on Mediterranean bathyal floors and in both deep and shallow (cold) waters of the East Atlantic (Vacelet & Boury-Esnault, 1996; Aguilar *et al.*, 2011; Chevaldonné *et al.*, 2015). The French and Croatian submarine caves where this species was originally discovered show a descending topography, and a deep submarine canyon is found nearby. These exceptional circumstances enable the winter injection of cold, deep water (and accompanying propagules) into these caves, where it remains trapped, enabling deep-water forms to thrive (Vacelet & Boury-Esnault, 1996; Bakran-Petricioli *et al.*, 2007).

The case of the two previously known anchialine cave polynoids, *Pelagomacellicephala iliffei* from the Bahamas archipelago and *Gesiella jameensis* from the Canary Islands, might lend support to the alternative Fuchs' (1894) hypothesis (see Gonzalez *et al.*, 2017, 2018a, 2021). The caves these taxa inhabit remain comparatively warm, but each represents a monotypic genus; molecular phylogenetic analyses place them as sister taxa within the exclusively deep-sea subfamily Macellicephalinae (Fig. 2; Gonzalez *et al.*, 2018b). They might be relics of a Tethyan bathyal fauna that penetrated the shallow-water crevicular environment before the aperture of the Atlantic, to end up separated by plate tectonic displacements at each side of the ocean (Iliffe *et al.*, 1984; Stock, 1986). But, Gonzalez *et al.* (2017) dated the divergence between *Pelagomacellicephala iliffei* and *Gesiella jameensis* at between 44.48 and 67.55 Mya based on molecular clock estimations. This age falls short compared to the assumed age for the establishment of deep water conditions between both shores of the Atlantic (95–110 Mya; Jones *et al.*, 1995), and thus does not support the involvement of vicariance in the origin of these two sister taxa.

The origin of *Pollentia perezi* remains unknown. It might be an ordinary marine species whose presence in the cave was accidental. However, the Balearic polychaete fauna is relatively well known (Barnich & Fiege, 2000; Fernández, 2002; Núñez *et al.*, 2011), and a large polynoid with such extraordinary morphological features is unlikely to pass unnoticed. Furthermore, depigmentation, lack of eyes, elongation of parapodial sensory appendages and swimming habits all point to a species remarkably adapted to the cave environment rather than to an ordinary shallow-water taxon (Gonzalez *et al.*, 2018b).

The new taxon does not seem to be a primary deep-water form like the cladorhicid sponge mentioned above. The cave waters it dwells in remain at > 16 °C all year round, compared with the 12–13 °C of western

Mediterranean bathyal depths (Vargas-Yáñez *et al.*, 2017), whereas the coastal waters adjacent to the cave can reach 28 °C in summer. Furthermore, the cave is located on a portion of coast facing a broad shelf (it lies ~15 km from the closest 100 m isobath, and 35 km from the 200 m isobath; see Fig. 1). Thus, there is no evident easy way for a deep-water taxon to reach the cave unless its life cycle includes a planktonic, dispersive larval stage. The reproductive strategy of the new species remains unknown; not even the gametes were observed in the examined specimens. Most Polynoidae have a life cycle involving a planktonic stage, either planktotrophic or lecitotrophic (e.g. Britayev, 1991; Giangrande, 1997; Pernet, 2000; Eckelbarger *et al.*, 2005). However, brooding has also been reported to occur in some species (e.g. Daly, 1972; Britayev & Belov, 1994; Gambi *et al.*, 2001). The reproductive mode of *Pelagomacellicephala* and *Gesiella*, the other two cave-dwelling polynoids, also remains unknown (A. Martínez, pers. comm). In any event, these larvae had to cope with the temperature barrier set between both environments.

Regarding conservation issues, *Pollentia perezi* most probably occurs elsewhere in subterranean habitats along the littoral zone of Mallorca and Menorca. The cave, representing the only known locality for the species, was completely emergent and located ~25 km inland as recently as at the Last Glacial Maximum (~21 000 years ago), when mean global sea level was ~134 m below its current level (Lambeck *et al.*, 2014). It is worth mentioning that the cave harbours, aside from the new polynoid, the second population known of the stygobiont cirolanid isopod *Metacirolana ponsi* Jaume & Garcia, 1992, known until now only from its type locality on Cabrera Island (off the south coast of Mallorca), and also the third population known of the stygobiont mysid *Burrimysis palmeri* Jaume & Garcia, 1993, initially recorded in the same cave on Cabrera and recently at another cave on the nearby south coast of Mallorca (see Fig. 1). *Metacirolana ponsi* and *Burrimysis palmeri* are Balearic endemics that occur exclusively in full-strength marine water layers of anchialine caves, and their presence in the Alcúdia cave suggests the existence of a crevicular continuum along the borders of the Mallorca plus Menorca promontory. This permanently dark network of apparently stagnant marine waters would enable the dispersal of so-called 'thalasso-stygobionts' (*sensu* Notenboom, 1991), thus explaining the apparent punctuated distribution pattern shown by these taxa.

ACKNOWLEDGEMENTS

We are grateful to Joan Pérez and other members of Societat Espeleològica Balear for collecting the specimens. Miquel A. Gual (WhiteLife Photography) provided some of the images of the new taxon. Maël Grosse helped with the sequencing of the DNA fragments. Conrad Helm confirmed that the pigmented structure visible in the prostomium of the new taxon is the brain. Three anonymous reviewers made useful comments and suggestions that greatly helped to improve the manuscript. M.C. was funded by the Ramón y Cajal programme (RYC-2016-20799) funded by Spanish Ministerio de Economía, Industria y Competitividad (MINECO), Agencia Estatal de Investigación, Govern de les Illes Balears and the European Social Fund.

REFERENCES

Aguilar R, **López Correa M**, **Calcinai B**, **Pastor X**, **de la Torriente A**, **Garcia S. 2011.** First records of *Asbestopluma hypogea* Vacelet and Boury-Esnault, 1996 (Porifera, Demospongiae Cladorhizidae) on seamounts and in bathyal settings of the Mediterranean Sea. *Zootaxa* **2925:** 33–40.

Allentoft-Larsen MC, **Gonzalez BC**, **Daniels J**, **Katija K**, **Osborn K**, **Worsaae K. 2021.** Muscular adaptations in swimming scale worms (Polynoidae, Annelida). *Royal Society Open Science* **8:** 210541.

Apakupakul K, **Siddall ME**, **Burreson EM. 1999.** Higher level relationships of leeches (Annelida: Clitellata: Euhirudinea) based on morphology and gene sequences. *Molecular Phylogenetics and Evolution* **12:** 350–359.

Bakran-Petricioli T, **Vacelet J**, **Zibrowius H**, **Petricioli D**, **Chevaldonné P**, **Rada T. 2007.** New data on the distribution of the 'deep-sea' sponges *Asbestopluma hypogea* and *Oopsacas minuta* in the Mediterranean Sea. *Marine Ecology* **28** (Suppl. 1): 10–23.

Barnich R, **Fiege D. 2000.** Revision of the Mediterranean species of *Harmothoe* Kinberg, 1856 and *Lagisca* Malmgren, 1865 (Polychaeta: Polynoidae: Polynoinae) with descriptions of a new genus and a new species. *Journal of Natural History* **34:** 1889–1938.

Bonifácio P, **Menot L. 2019.** New genera and species from the Equatorial Pacific provide phylogenetic insights into deep-sea Polynoidae (Annelida). *Zoological Journal of the Linnean Society* **185:** 555–635.

Briggs JC. 1995. *Global biogeography. Developments in palaeontology and stratigraphy*, *vol.* **14**. Amsterdam: Elsevier.

Britayev TA. 1991. Life cycle of the symbiotic scaleworm *Arctonoe vittata* (Polychaeta: Polynoidae). *Ophelia* **5** (Suppl): 305–312.

Britayev TA, **Belov VV. 1994.** Age determination of Polynoidae polychaetes based on growth lines on the jaws. *Hydrobiological Journal* **30:** 53–60.

Chevaldonné P, **Jollivet D**, **Feldman RA**, **Desbruyères D**, **Lutz RA**, **Vrijenhoek RC. 1998.** Commensal scale-worms of the genus *Branchipolynoe* (Polychaeta: Polynoidae) at deep-sea hydrothermal vents and cold seeps. *Cahiers de Biologie Marine* **39:** 347–350.

Chevaldonné P, **Pérez T**, **Crouzet JM**, **Bay-Nouailhat W**, **Bay-Nouailhat A**, **Fourt M**, **Almón B**, **Pérez J**, **Aguilar R**, **Vacelet J. 2015.** Unexpected records of 'deep-sea' cavernicolous sponges *Asbestopluma hypogea* in the shallow NE Atlantic shed light on new conservation issues. *Marine Ecology* **36:** 475–484.

Dales RP, **Peter G. 1972.** A synopsis of the pelagic Polychaeta. *Journal of Natural History* **6:** 55–92.

Daly JM. 1972. The maturation and breeding biology of *Harmothoe imbricata* (Polychaeta: Polynoidae). *Marine Biology* **12:** 53–66.

De Pinna MCC. 1991. Concepts and tests of homology in the cladistic paradigm. *Cladistics* **7:** 367–394.

Eckelbarger K, **Watling L**, **Fournier H. 2005.** Reproductive biology of the deep-sea polychaete *Gorgoniapolynoe caeciliae* (Polynoidae), a commensal species associated with octocorals. *Journal of the Marine Biological Association of the United Kingdom* **85:** 1425–1433.

Edgar RC. 2004. MUSCLE: multiple sequence alignment with high accuracy and high throughput. *Nucleic Acids Research* **32:** 1792–1797.

Fernández J. 2002. Noticia de nuevos taxones para la ciencia en el ámbito Ibero-Balear y Macaronésico. *Graellsia* **58:** 97–124.

Fuchs T. 1894. Ueber Tiefseetiere in Höhlen. *Annalen des KK Naturhistorischen Hofmuseums in Wien* **9:** 54–55.

Gambi M, **Patti F**, **Micaletto G**, **Giangrande A. 2001.** Diversity of reproductive features in some Antarctic polynoid and sabellid polychaetes, with a description of *Demonax polarsterni* sp. n. (Polychaeta, Sabellidae). *Polar Biology* **4:** 883–891.

Geller J, **Meyer C**, **Parker M**, **Hawk H. 2013.** Redesign of PCR primers for mitochondrial cytochrome *c* oxidase subunit I for marine invertebrates and application in all-taxa biotic surveys. *Molecular Ecology Resources* **13:** 851–861.

Giangrande A. 1997. Polychaete reproductive patterns, life cycles and life histories: an overview. In: Ansel AD, GibsonRN, Barnes M, eds. *Oceanography and Marine Biology: an Annual Review*, vol. **35**. London: UCL Press, 323–338.

Gonzalez BC, **Martínez A**, **Borda E**, **Iliffe TM**, **Eibye-Jacobsen D**, **Worsaae K. 2018a.** Phylogeny and systematics of Aphroditiformia. *Cladistics* **34:** 225–259.

Gonzalez BC, **Martínez A**, **Borda E**, **Iliffe T**, **Fontaneto D**, **Worsae K. 2017.** Genetic spatial structure of an anchialine cave annelid indicates connectivity within - but not between - islands of the Great Bahama Bank. *Molecular Phylogenetics and Evolution* **109:** 259–270.

Gonzalez BC, **Martínez A**, **Worsaae K**, **Osborn KJ. 2021.** Morphological convergence and adaptation in cave and pelagic scale worms (Polynoidae, Annelida). *Scientific Reports* **11:** 10718.

Gonzalez BC, **Worsaae K**, **Fontaneto D**, **Martínez A. 2018b.** Anophthalmia and elongation of body appendages in cave scale worms (Annelida: Aphroditiformia). *Zoologica Scripta* **47:** 106–121.

Gouy M, **Guindon S**, **Gascuel O. 2010.** SeaView version 4: a multiplatform graphical user interface for sequence alignment and phylogenetic tree building. *Molecular Biology and Evolution* **27:** 221–224.

Hart CW Jr, **Manning RB**, **Iliffe TM**. **1985.** The fauna of Atlantic marine caves: evidence of dispersal by sea floor spreading while maintaining ties to deep waters. *Proceedings of the Biological Society of Washington* **98:** 288–292.

Hartman O. 1939. Polychaetous annelids. Part I. Aphroditidae to Pisionidae. *Allan Hancock Pacific Expeditions* **7:** 1–156.

Hartmann-Schröder G. 1974. Die unterfamilie Macellicephalinae Hartmann-Schröder, 1971 (Polynoidae, Polychaeta). Mit Beschriebung einer neuer Art, *Macellicephala jameensis*, n. sp., aus einen hohlengewasser von Lanzarote (Kanarische Inseln). *Mitteilungen aus dem Hamburgischen Zoologischen Museum und Institut* **71:** 75–85.

Hutchings PA, **Murray A. 1984.** Taxonomy of polychaetes from the Hawkesbury River and the southern estuaries of New South Wales, Australia. *Records of the Australian Museum* **3:** 1–118.

Iliffe TM. 2000. Anchialine cave ecology. In: Wilkens H, Culver DC & Humphreys WH, eds. *Ecosystems of the world. 30. Subterranean ecosystems*. Amsterdam: Elsevier Science, 59–76.

Iliffe TM, **Wilkens H**, **Parzefall J**, **Williams, D. 1984.** Marine lava cave fauna: composition, biogeography, and origins. *Science* **225:** 309–311.

Jaume D, **Garcia L. 1992.** A new *Metacirolana* (Crustacea: Isopoda: Cirolanidae) from an anchihaline cave lake on Cabrera (Balearic Islands). *Stygologia* **7:** 179–186.

Jaume D, **Garcia L. 1993.** *Burrimysis palmeri*, a new genus and species of Heteromysini (Crustacea: Mysidacea) from an anchihaline cave lake of Cabrera (Balearic Islands, Mediterranean). *Bijdragen tot de Dierkunde* **62:** 227–235.

Jones, EJW, **Cande SC**, **Spathopoulos F. 1995.** Evolution of a major oceanographic pathway: the equatorial Atlantic. *Geological Society, London, Special Publications*, **90:** 199–213.

Jumars PA, **Dorgan KM**, **Lindsay SM. 2015.** Diet of worms emended: an update of polychaete feeding guilds. *Annual Review of Marine Science* **7:** 497–520.

Katoh K, **Standley DM. 2013.** MAFFT multiple sequence alignment software version 7: improvements in performance and usability. *Molecular Biology and Evolution* **30:** 772–780.

Kearse M, **Moir R**, **Wilson A**, **Stones-Havas S**, **Cheung M**, **Sturrock S**, **Buxton S**, **Cooper A**, **Markowitz S**, **Duran C**, **Thierer T**, **Ashton B**, **Meintjes P**, **Drummond A. 2012.** Geneious Basic: an integrated and extendable desktop software platform for the organization and analysis of sequence data. *Bioinformatics* **28:** 1647–1649.

Lambeck K, **Rouby H**, **Purcell A**, **Sun Y**, **Sambridge M. 2014.** Sea level and global ice volumes from the Last Glacial Maximum to the Holocene. *Proceedings of the National Academy of Sciences of the United States of America* **111:** 15296–15303.

Lê HLV, **Lecointre G**, **Perasso R. 1993.** A 28S rRNA-based phylogeny of the Gnathostomes: first steps in the analysis of conflict and congruence with morphologically based cladograms. *Molecular Phylogenetics and Evolution* **2:** 31–51.

Martin D, **Aguado MT**, **Álamo MAF**, **Britayev TA**, **Böggemann M**, **Capa M**, **Faulwetter S**, **Fukuda MV**, **Helm C**, **Varella Petti MA**, **Ravara A**, **Teixeira MA. 2021.** On the diversity of Phyllodocida (Annelida: Errantia), with a focus on Glyceridae, Goniadidae, Nephtyidae, Polynoidae, Sphaerodoridae, Syllidae, and the holoplanktonic families. *Diversity* **13:** 131.

Martin D, **Britayev TA. 2018.** Symbiotic polychaetes revisited: an update of the known species and relationships (1998–2017). In: Hawkins SJ, Evans AJ, Dale AC, Firth LB, Smith IP. *Oceanography and Marine Biology: Annual Review*, *vol.* **56**. Boca Raton: CRC Press, 371–447.

McIntosh WC. 1885. Report on the Annelida Polychaeta collected by H.M.S. Challenger during the years 1873-1876. Report on the Scientific Results of the Voyage of H.M.S. Challenger during the years 1873–76. *Zoology* **12**(part 34): 1–554.

Medlin L, **Elwood HJ**, **Stickel S**, **Sogin ML. 1988.** The characterization of enzymatically amplified eukaryotic 16S-like rRNA-coding regions. *Gene* **71:** 491–499.

Minh BQ, **Hahn MW**, **Lanfear R. 2020.** New methods to calculate concordance factors for phylogenomic datasets. *Molecular Biology and Evolution* **37:** 2727–2733.

Monro CCA. 1939. Polychaeta. B.A.N.Z. *Antarctic Research Expedition Reports, Series B: Zoology and Botany* **4:** 87–156.

Moore JP. 1910. The polychaetous annelids dredged by the U.S.S. Albatross off the coast of Southern California in 1904, 2. Polynoidae, Aphroditidae and Segaleonidae (sic). *Proceedings of the Academy of Natural Sciences of Philadelphia* **62:** 328–402.

Norlinder E, **Nygren A**, **Wiklund H**, **Pleijel F. 2012.** Phylogeny of scale-worms (Aphroditiformia, Annelida), assessed from 18SrRNA, 28SrRNA, 16SrRNA, mitochondrial cytochrome c oxidase subunit I (COI), and morphology. *Molecular Phylogenetics and Evolution* **65:** 490–500.

Notenboom J. 1991. Marine regressions and the evolution of groundwater dwelling amphipods (Crustacea). *Journal of Biogeography* **18:** 437–454.

Núñez J, **Barnich R**, **Santos L**, **Maggio Y. 2011.** Poliquetos escamosos (Annelida, Polychaeta) colectados en las campañas 'Fauna II, III, IV' (Proyecto 'Fauna Ibérica') y catálogo de las especies conocidas para el ámbito íbero-balear. *Graellsia* **67:** 187–197.

Pallas PS. 1766. Miscellanea zoologica. Quibus novae imprimis atque obscurae animalium species describuntur et observationibus iconibusque illustrantur. Petrum van Cleef. Hagí Comitum, 224 pp.

Palumbi SR. 1996. Nucleic acids II: the polymerase chain reaction. In: Hillis DM, Mable BK, Moritz C, eds. *Molecular systematics*. Sunderland: Sinauer, 205–247.

Pernet B. 2000. Reproduction and development of three symbiotic scale worms (Polychaeta: Polynoidae). *Invertebrate Biology* **119:** 45–57.

Pettibone MH. 1967. Some bathyal Polynoids from central and northeastern Pacific (Polychaeta: Polynoids). *Proceedings of the United States National Museum* **121:** 1–15.

Pettibone MH. 1969. Revision of the aphroditoid polychaetes of the family Eulepethidae Chamberlin (= Eulepidinae Darboux; = Pareulepidae Hartman). *Smithsonian Contributions to Zoology* **14:** 1–44.

Pettibone MH. 1976. Revision of the genus *Macellicephala* McIntosh and the subfamily Macellicephalinae Hartmann-Schröder (Polychaeta: Polynoidae). *Smithsonian Institution Contributions to Zoology* **229:** 1–71.

Pettibone MH. 1984. Two new species of *Lepidonotopodium* (Polychaeta: Polynoidae: Lepidonotopodinae) from hydrothermal vents off the Galapagos and East Pacific Rise at 21°N. *Proceedings of the Biological Society of Washington* **97:** 849–863.

Pettibone MH. 1985. Polychaete worms from a cave in the Bahamas and from experimental wood panels in deep water of the North Atlantic (Polynoidae: Macellicephalinae, Harmothoinae). *Proceedings of the Biological Society of Washington* **98:** 127–149.

Pettibone MH. 1997. Revision of the scaleworm genus *Eulagisca* McIntosh (Polychaeta: Polynoidae) with the erection of the subfamily Eugaliscinae and the new genus *Pareulagisca*. *Proceedings of the Biological Society of Washington* **110:** 537–551.

Racovitza EG. 1907. Biospéologica, I. Essai sur les problèmes biospéologiques. *Archives de Zoologie Expérimentale et Générale* **6:** 371–488.

Read G, **Fauchald K. 2021.** Polynoidae Kinberg, 1856. World Polychaeta Database. Available at: https://www.marinespecies.org/aphia.php?p=taxdetails&id=939

Ronquist F, **Huelsenbeck JP. 2003.** MRBAYES 3: Bayesian phylogenetic inference under mixed models. *Bioinformatics* **19:** 1572–1574.

Sars M. 1835. Beskrivelser og Iagttagelser over nogle moerkelige eller nye i Havet ved den Bergenske Kyst levende Dyr af Polypernes, Acalephernes, Radiaternes, Annelidernes og Molluskernes classer, med en kort Oversigt over de hidtil af Forfatteren sammesteds fundne Arter og deres Forekommen. Thorstein Hallagers Forlag hos Chr. Dahl, R.S., 81 pp.

Sela I, **Ashkenazy H**, **Katoh K**, **Pupko T. 2015.** GUIDANCE2: accurate detection of unreliable alignment regions accounting for the uncertainty of multiple parameters. *Nucleic Acids Research* **43:** W7–W14.

Shimodaira H. 2002. An approximately unbiased test of phylogenetic tree selection. *Systematic Biology* **51:** 492–508.

Stock JH. 1986. Deep sea origin of cave faunas: an unlikely supposition. *Stygologia* **2:** 105–111.

Struck TH, **Purschke G**, **Halanych KM. 2005.** A scaleless scale worm: Molecular evidence for the phylogenetic placement of *Pisione remota* (Pisionidae, Annelida). *Marine Biology Research* **1:** 243–253.

Suárez R. 1993. Aportació al coneixement espeleològic del Cap des Pinar a Alcúdia (Mallorca). *Endins* **19:** 25–28.

Sui J, **Li X. 2017.** A new species and new record of deep-sea scale-worms (Polynoidae: Polychaeta) from the Okinawa Trough and the South China Sea. *Zootaxa* **4238:** 562–570.

Tabei Y, **Kiryu H**, **Kin T. Asai K. 2008.** A fast structural multiple alignment method for long RNA sequences. *BMC Bioinformatics* **9:** 1–17.

Talavera G, **Castresana J. 2007.** Improvement of phylogenies after removing divergent and ambiguously aligned blocks from protein sequence alignments. *Systematic Biology* **56:** 564–77.

Vacelet J, **Boury-Esnault N. 1996.** A new species of carnivorous sponge (Demospongiae: Cladorhizidae) from a Mediterranean cave. *Bulletin de l'Institut Royal des Sciences Naturelles de Belgique, Biologie* **66:** 109–115.

Vargas-Yáñez M, **García-Martínez MC**, **Moya F**, **Balbín R**, **López-Jurado JL**, **Serra M**, **Zunino P**, **Pascual J**, **Salat J. 2017.** Updating temperature and salinity mean values and trends in the western Mediterranean: the RADMED Project. *Progress in Oceanography* **157:** 27–46.

Wehe T. 2006. Revision of the scale worms (Polychaeta: Aphroditoidea) occurring in the seas surrounding the Arabian Peninsula. Part I: Polynoidae. *Fauna of Arabia* **22:** 23–197.

Wiklund H, **Nygren A**, **Pleijel F**, **Sundberg P. 2005.** Phylogeny of Aphroditiformia (Polychaeta) based on molecular and morphological data. *Molecular Phylogenetics and Evolution* **37:** 494–502.

Wu X, **Zhan Z**, **Xu K. 2019.** Two new and two rarely known species of *Branchinotogluma* (Annelida: Polynoidae) from deep-sea hydrothermal vents of the Manus Back-Arc basin, with remarks on the diversity and biogeography of vent polynoids. *Deep Sea Research Part I: Oceanographic Research Papers* **149:** 103051.

Zhang Y, **Sun J**, **Rouse GW**, **Wiklund H**, **Pleijel F**, **Watanabe HK**, **Chen C**, **Qian P**, **Qiu, JW. 2018.** Phylogeny, evolution and mitochondrial gene order rearrangement in scale worms (Aphroditiformia, Annelida). *Molecular Phylogenetics and Evolution* **125:** 220–231.

SUPPORTING INFORMATION

Supporting Information, S1. Complete dataset alignment of four markers with MUSCLE and default parameters.

Supporting Information, S2. Complete dataset alignment of four markers (18S rRNA, 28S rRNA, 16S rRNA and *COI*) with MUSCLE and default parameters. Non-conserved blocks were removed in GBLOCKS in low stringent conditions.

Supporting Information, S3. Complete dataset alignment of four markers, with *COI* with MUSCLE and default parameters, and 16S rRNA, 28S rRNA and 18SrRNA with MAFFT and *xinsi* strategy.

Supporting Information, S4. Complete dataset alignment of four markers, with *COI* with MUSCLE and default parameters and 16S rRNA, 28S rRNA, and 18SrRNA with MAFFT *xinsi* strategy. Non-conserved blocks were removed in GBLOCKS in low stringent conditions.

Supporting Information, S5. Complete dataset alignment of four markers, with *COI* with MUSCLE and default parameters, and 16S rRNA, 28S rRNA and 18SrRNA with GUIDANCE2.

Supporting Information, S6. Complete dataset alignment of four markers, with *COI* with MUSCLE and default parameters, and 16S rRNA, 28S rRNA and 18SrRNA with GUIDANCE2 but only with fully supported aligned sites.

Supporting Information, Figure S7. Number of positions of each marker included in analyses depending on the alignment strategy followed.

Supporting Information, S8. Reduced dataset alignment of four markers (18S rRNA, 28S rRNA, 16S rRNA and *COI*) with MUSCLE and default parameters. Non-conserved blocks were removed in GBLOCKS in low stringent conditions.

Supporting Information, S9. Reduced dataset alignment of four markers, with *COI* with MUSCLE and default parameters, and 16S rRNA, 28S rRNA and 18SrRNA with MAFFT *xinsi* strategy. Non-conserved blocks were removed in GBLOCKS in low stringent conditions.

Supporting Information, S10. Reduced dataset alignment of four markers, with *COI* with MUSCLE and default parameters, and 16S rRNA, 28S rRNA and 18SrRNA with GUIDANCE2.

Supporting Information, Figure S11. Phylogenetic hypotheses of Polynoidae, with all alignments of the four concatenated genetic markers (18S rRNA, 28S rRNA, 16S rRNA and *COI*) inferred from the maximum likelihood analysis, and GUIDANCE2 and complete taxon list before and after removing poorly aligned positions and divergent regions.

Supporting Information, Figure S12. Phylogenetic hypotheses of Polynoidae, with all alignments of the four concatenated genetic markers (18S rRNA, 28S rRNA, 16S rRNA and *COI*) inferred from the maximum likelihood analysis, and GUIDANCE2 and reduced taxon list before and after removing poorly aligned positions and divergent regions.

Supporting Information, Figure S13. Approximately unbiased test of phylogenetic tree selection (AU-test) of complete datasets.

Supporting Information, Figure S14. Approximately unbiased test of phylogenetic tree selection (AU-test) of reduced datasets.

Supporting Information, Video S15. Videoclip showing the bottom of the cave where *Pollentia perezi* was discovered. The paratype takes off and swims before reaching the bottom again.

Supporting Information, Video S16. Videoclip showing holotype of *Pollentia perezi* crawling in a glass container.